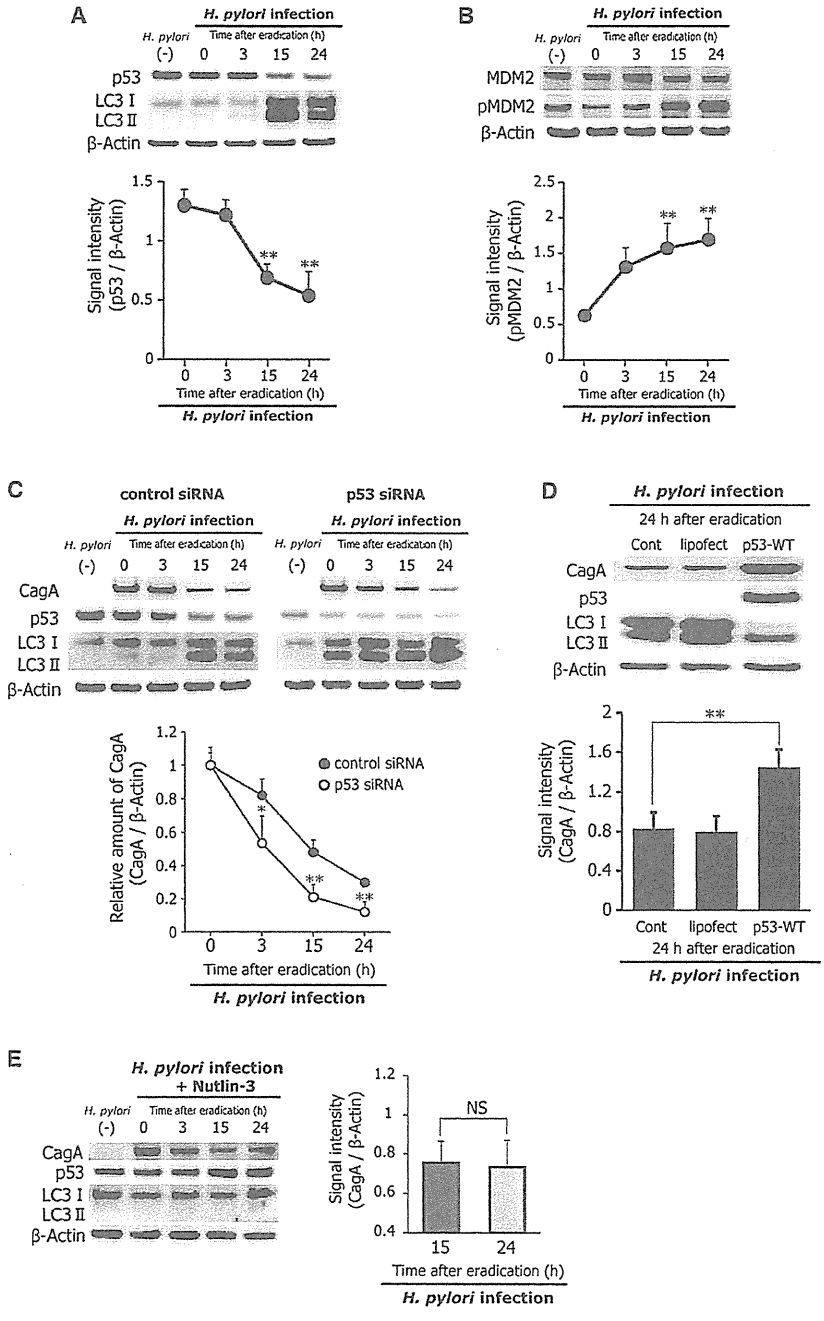


**Figure 4. Autophagy, Causing CagA Degradation, Is Induced through MDM2-Mediated p53 Degradation**

(A) AGS cells infected with *H. pylori* (s1m1VacA) for 5 hr were incubated in a medium containing antibiotic for the indicated time, and p53 expression and LC3-I to LC3-II conversion were examined. Data represent the mean ± SD of three independent assays; **p < 0.01, compared to AGS cells at 0 hr after *H. pylori* (s1m1VacA) eradication.

(B) AGS cells infected with *H. pylori* (s1m1VacA) for 5 hr were incubated in a medium containing antibiotic for the indicated times, and the levels of MDM2 and phosphorylated-MDM2 (pMDM2) were examined. Data represent the mean ± SD of three independent assays; **p < 0.01, compared to AGS cells at 0 hr after *H. pylori* (s1m1VacA) eradication.

(C) After AGS cells were transfected with control siRNA or p53 siRNA, cells infected with *H. pylori* (s1m1VacA) for 5 hr were incubated in a medium containing antibiotic for the indicated times, and the levels of CagA, p53 expression, and LC3-I to LC3-II conversion were examined. Data represent the mean ± SD of three independent assays; **p < 0.01, compared to AGS cells transfected with control siRNA at each time point after *H. pylori* (s1m1VacA) eradication.

(D) KATOIII cells were transfected with the pCMV-Neo-Bam WT *p53* plasmid (p53-WT) or without (Cont). Each cell after *H. pylori* (s1m1VacA) infection for 5 hr was incubated in a medium containing antibiotic for the indicated times. CagA levels and LC3-I to LC3-II conversion were examined. Data represent the mean ± SD of three independent assays; **p < 0.01; lipofect indicates KATOIII cells treated with only Lipofectamine 2000.

(E) AGS cells infected with *H. pylori* (s1m1VacA) for 5 hr were incubated in a medium containing antibiotic for the indicated times with 10 μM nutlin-3, and the levels of CagA, p53 expression, and LC3-I to LC3-II conversion were examined. Data represent the mean ± SD of three independent assays; NS, not significant. See also Figure S2.

p53-knockdown using small interfering RNAs (siRNAs) accelerated LC3-I to LC3-II conversion, thereby enhancing CagA degradation in AGS cells after *H. pylori* ATCC700392 (s1m1VacA) infection (Figure 4C). Moreover, in KATOIII cells, which are genetically deficient of p53 ($p53^{-/-}$ KATOIII cells), LC3-I to LC3-II conversion was clearly detected at 24 hr after the eradication of *H. pylori* ATCC700392 (s1m1VacA), and intracellular CagA levels were significantly decreased, as compared with $p53^{-/-}$ KATOIII cells transfected with the WT *p53* expression plasmid (Figure 4D). In addition, we examined the effect of nutlin-3—an inhibitor of MDM2-phosphorylation—on CagA stability. Treatment with 10 μM nutlin-3 repressed p53 downregulation and LC3-I to LC3-II conversion (Figure 4E), resulting in the inhibition of CagA degradation (Figure 4E). These results show that p53 downregulation, through the acceleration of MDM2-phosphorylation by m1VacA, induces autophagy, causing CagA degradation.

## ROS Accumulation Is Necessary for the Induction of Autophagy, Causing CagA Degradation

An accumulation of intracellular ROS induces autophagy, and the generation of intracellular ROS is enhanced in gastric epithelial cells during *H. pylori* infection (Ding et al., 2007). We hypothesized that the enhanced generation of intracellular ROS participates in induction of autophagy, causing CagA

degradation. AGS cells at 15 and 24 hr after the eradication of infected *H. pylori* were analyzed using fluorescence microscopy and flow cytometry after staining with CM-$H_2$DCFDA, an ROS-sensitive fluorescent probe. Hydrolyzed CM-$H_2$DCFDA is oxidized to dichlorofluorescein (DCF) by intracellular ROS (Suzuki et al., 1994). DCF fluorescence was apparent in AGS cells at 15 and 24 hr after the eradication of *H. pylori* ATCC700392 (s1m1VacA), as compared with AGS cells without *H. pylori* exposure (Figure 5A). The intensity of DCF fluorescence in AGS cells at 15 and 24 hr after the eradication of *H. pylori* ATCC700392 (s1m1VacA) was significantly increased, as compared to AGS cells without *H. pylori* exposure (Figure 5B). Conversely, in AGS cells after *H. pylori* F57 (VacA-negative), ot210 (s1m2VacA), or SS1 (s2m2VacA) infection, no increase in DCF fluorescence was observed (Figure S3A). These results show that the accumulation of intracellular ROS was enhanced during the induction of autophagy.

NADPH oxidase (NOX)-generated ROS is a key regulator of autophagy (Huang et al., 2009), while mitochondrial-superoxide ($O_2^-$) production is involved in the induction of autophagy (Scherz-Shouval and Elazar, 2007). To identify the source of enhanced ROS generation associated with the induction of autophagy through p53 downregulation, we examined the effects of an NOX inhibitor (acetovanillone), an MnSOD mimic compound (MnTMPyP), and N-acetylcysteine (NAC). p53 downregulation was not inhibited by 250 μM acetovanillone or 20 μM MnTMPyP; therefore, LC3-I to LC3-II conversion was not repressed (Figure 5C). Conversely, p53 downregulation was inhibited by treatment with 10 mM NAC, and LC3-I to LC3-II conversion was repressed (Figure 5C). Moreover, intracellular CagA levels were significantly increased by treatment of AGS cells with 10 mM NAC at 24 hr after the eradication of *H. pylori* ATCC700392 (s1m1VacA) (Figure 5D). These results show that the accumulation of intracellular ROS is necessary for induction of autophagy, causing CagA degradation, independent of NOX- and mitochondria-associated ROS generation.

Administration of NAC, a cysteine prodrug, replenishes intracellular GSH levels; therefore, NAC has been used to treat GSH deficiency (Atkuri et al., 2007). We hypothesized that the accumulation of intracellular ROS during the induction of autophagy was caused by decreased GSH levels. To prove this, we examined the change of GSH levels in AGS cells after *H. pylori* ATCC700392 (s1m1VacA) infection. Intracellular GSH levels in AGS cells at 15 and 24 hr after the eradication of *H. pylori* ATCC700392 (s1m1VacA) were significantly decreased, as compared to AGS cells without *H. pylori* exposure (Figure 5E). Moreover, intracellular GSH levels in AGS and CagA-expressing WT-A10 cells were significantly decreased by m1VacA in a dose-dependent manner (Figure 5F). In AGS cells at 15 and 24 hr after the eradication of *H. pylori* ATCC700392 (s1m1VacA), intracellular GSH was decreased, as compared to cells at 15 and 24 hr after eradication of *H. pylori* F57 (VacA-negative), ot210 (s1m2VacA), or SS1 (s2m2VacA) (Figure S3B). Moreover, intracellular GSH levels in AGS and CagA-expressing WT-A10 cells were not decreased by treatment with m2VacA (Figure S3C). These results show that the accumulation of intracellular ROS associated with the induction of autophagy was induced by decreased GSH levels caused by m1VacA. Next, to provide the relevance of LRP1 in the reduction of intracellular GSH levels, we measured intracellular GSH levels in specific LRP1-knockdown AGS cells; they were significantly increased at 15 or 24 hr after the eradication of *H. pylori* ATCC700392 (s1m1VacA), as compared with those in AGS cells transfected with control siRNA (Figure S3D). These results demonstrate that the binding of m1VacA to LRP1 is required for the reduction of intracellular GSH levels.

### Activation of the Akt Pathway Depends on the Accumulation of ROS for Autophagy Induction

Phosphorylated Akt enhances the ubiquitination-promoting function of MDM2 by phosphorylation, resulting in p53 downregulation (Ogawara et al., 2002). In addition, exogenous and endogenous ROS enhance Akt phosphorylation (Dong-Yun et al., 2003). We hypothesized that the accumulation of intracellular ROS by decreased GSH levels enhances Akt phosphorylation, leading to the induction of autophagy through p53 downregulation by the activation of MDM2. To investigate this hypothesis, we examined Akt phosphorylation in AGS cells after *H. pylori* ATCC700392 (s1m1VacA) infection. Although Akt expression was unaltered, the levels of phosphorylated Akt at Thr308 and Ser473 were significantly increased in AGS cells after *H. pylori* ATCC700392 (s1m1VacA) infection (Figure 6A). To examine whether Akt phosphorylation depends on the accumulation of intracellular ROS, we examined the effect of NAC on Akt phosphorylation. Treatment with 10 mM NAC inhibited Akt phosphorylation at Ser473, but not at Thr308 (Figure 6A); therefore, Akt phosphorylation at Ser473 was dependent on accumulation of intracellular ROS after *H. pylori* ATCC700392 (s1m1VacA) infection. In addition, although Akt phosphorylation at Thr308 was increased in AGS cells after *H. pylori* F57 (VacA-negative), ot210 (s1m2VacA), or SS1 (s2m2VacA) infection, Akt phosphorylation at Ser473 was not increased (Figure S4A). Moreover, Akt phosphorylation at Thr308 and Ser473 was not increased in CagA-expressing WT-A10 cells, suggesting that Akt phosphorylation was independent of intracellular CagA (Figure S4B).

To examine the relevance of Akt phosphorylation at Ser473 to the induction of autophagy, causing CagA degradation, we examined the effect of LY294002, an inhibitor of Akt phosphorylation, on the stability of intracellular CagA and autophagy induction. Ten micromolar LY294002 inhibited intracellular CagA degradation, the increase in pMDM2, and p53 downregulation (Figure 6B). As a result, LC3-I to LC3-II conversion in AGS cells at 15 and 24 hr after the eradication of *H. pylori* ATCC700392 (s1m1VacA) was repressed by LY294002 with reduced accumulation of LysoTracker Red (Figure 6C). These results suggest that enhanced Akt phosphorylation at Ser473 induced MDM2 phosphorylation, leading to the induction of autophagy and causing CagA degradation through p53 downregulation.

### Accumulation of Translocated CagA in CD44v9-Expressing Gastric Cancer Stem-like Cells

Intracellular CagA produced by m1VacA *H. pylori*, but not m2VacA *H. pylori*, was degraded by autophagy. Although some studies indicated that m1VacA *H. pylori* infection was at a greater risk of gastric cancer compared with m2VacA *H. pylori* infection (Basso et al., 2008; Miehlke et al., 2000), others have indicated that there is no correlation between virulence and the *vacA*

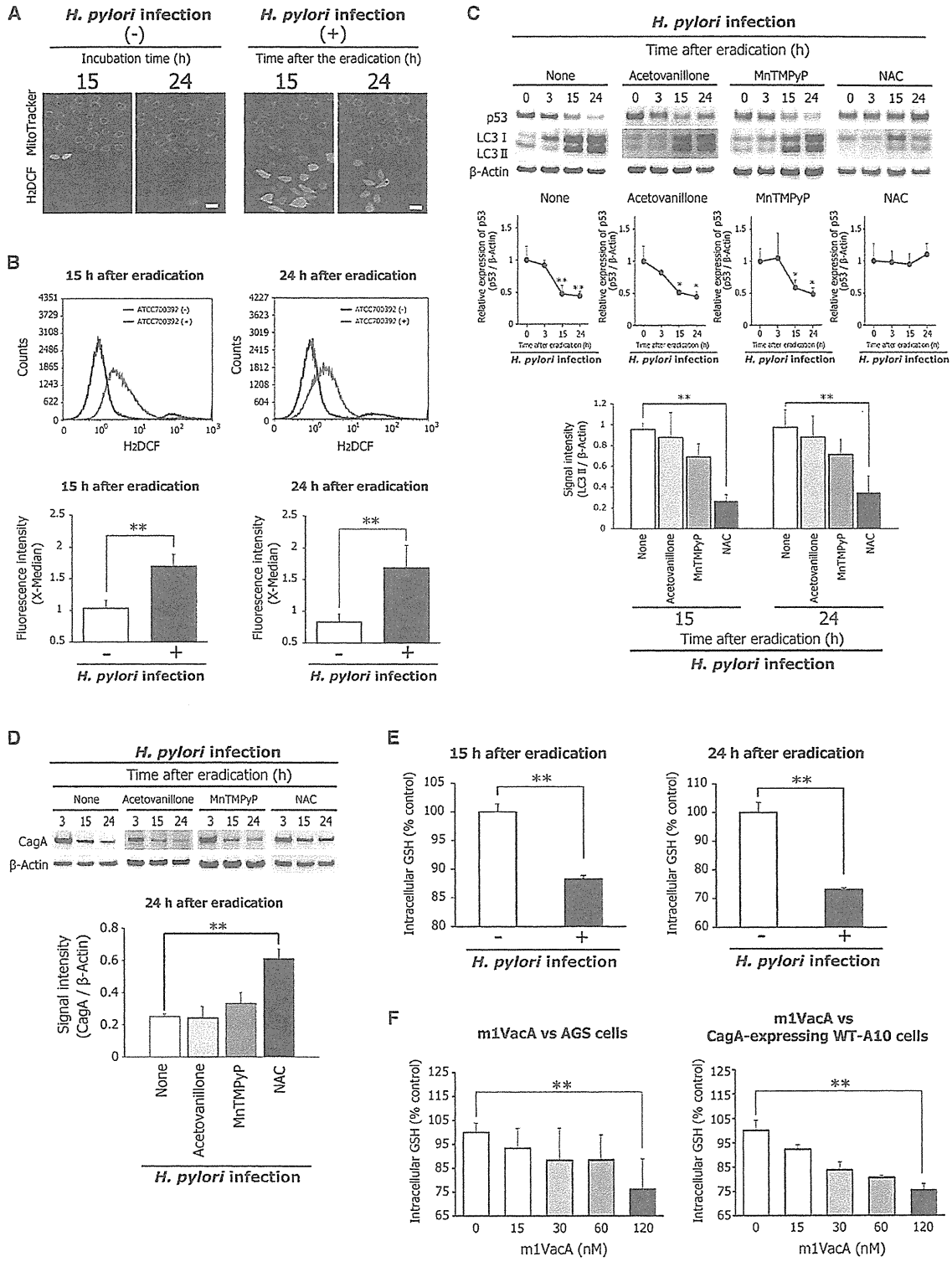


**Figure 5. Reduced Intracellular GSH Levels Trigger Autophagy, Causing CagA Degradation**

(A) AGS cells at 24 hr after *H. pylori* (s1m1VacA) eradication were stained with CM-$H_2$DCFDA and MitoTracker Red FM and examined by fluorescence microscopy. Scale bar = 50 μm.

(B) Flow cytometry of AGS cells at 15 and 24 hr after *H. pylori* (s1m1VacA) eradication. $H_2$DCF fluorescence intensity was determined by using analysis software. Data represent the mean ± SD of three independent assays; **p < 0.01.

genotype (Marshall et al., 1999; Yamaoka et al., 1998). In fact, m1 and m2 VacA strains are both observed in gastric cancer patients (Wang et al., 1998). From these reports, we hypothesized that there was a characteristic alteration in host cell associated with the inhibition of autophagy, which led to the accumulation of intracellular CagA. CD44v9-expressing gastric cancer cells are resistant to ROS, supported by increased intracellular GSH synthesis (Ishimoto et al., 2011). We hypothesized that accumulation of intracellular CagA resulted from inhibiting autophagy induction in CD44v9-expressing cells. To prove this hypothesis, we prepared MKN28 mutant cells by transfection of CD44 standard form (CD44s)- or CD44v9-expression vectors into CD44-negative MKN28 cells (Ishimoto et al., 2011). CD44s or CD44v9 expression in MKN28 cells was confirmed using flow cytometry (Figure S5A). Intracellular GSH levels in MKN28 cells expressing CD44s were significantly increased in comparison to MKN28 cells, whereas GSH levels in MKN28 cells expressing CD44v9 were increased in comparison to MKN28 cells expressing CD44s (Figure S5B). These results were consistent with previous observations that CD44v9 expression increases cellular GSH contents through the promotion of xCT-mediated cystine uptake, and CD44s expression increases cellular GSH levels through the maintenance of pentose phosphate pathway (PPP) flux and consequent NADPH production (Tamada et al., 2012). Intracellular GSH levels in MKN28 cells expressing CD44v9 were not decreased at 15 or 24 hr after the eradication of *H. pylori* ATCC700392 (s1m1VacA), in contrast to the reduction of GSH levels in MKN28 cells expressing CD44s (Figure 7A). Intracellular CagA levels were significantly increased in MKN28 cells expressing CD44v9, as compared with those in MKN28 cells expressing CD44s (Figure 7B). In addition, the increase of Akt and MDM2 phosphorylation and p53 degradation were not observed in MKN28 cells expressing CD44v9 (Figure 7B). As a result, LC3-I to LC3-II conversion was repressed (Figure 7B) and LysoTracker signals were markedly decreased in MKN28 cells expressing CD44v9 (Figure 7C). These results suggest that intracellular CagA accumulated in cells expressing CD44v9 through the inhibition of autophagy. We then examined the effect of sulfasalazine, a potent xCT inhibitor, on the stability of intracellular CagA in MKN28 cells expressing CD44v9. Intracellular CagA levels were decreased by the application of sulfasalazine in a dose-dependent fashion (Figure 7D). Moreover, Akt and MDM2 phosphorylation was significantly increased, and p53 downregulation was induced by treatment with sulfasalazine (Figure 7D), resulting in a significant increase in the conversion of LC3-I to LC3-II (Figure 7D).

To assess the effect of CD44v9-expression on the accumulation of intracellular CagA in human gastric adenocarcinoma, endoscopically resected early gastric cancer tissue from four patients (case 1: 62-year-old female, well-differentiated adenocarcinoma, *H. pylori*-positive; case 2: 68-year-old male, well-differentiated adenocarcinoma, *H. pylori*-positive; case 3: 72-year-old male, well-differentiated adenocarcinoma, *H. pylori*-positive; case 4: 78-year-old male, well-differentiated adenocarcinoma, *H. pylori*-positive), with written informed consent, was used. Remarkable intracellular CagA staining was detected with an anti-CagA antibody in the CD44v9-positive cells in each gastric adenocarcinoma (Figure 7E). It was confirmed using an anti-*H. pylori* antibody that these CagA-stained patterns were different from *H. pylori*-specific staining (not CagA) (data not shown), suggesting that only transported CagA, but not the *H. pylori* itself, was detected in CD44v9-expressing gastric cancer tissue. Endoscopically resected early gastric cancer tissue from an *H. pylori*-negative patient (80-year-old female, well-differentiated adenocarcinoma), with written informed consent, was used as a CagA-negative control. In this specimen, intracellular CagA staining was not detected in either CD44v9-positive or CD44v9-negative cells (Figure S5C). In addition, we detected the intracellular CagA-negative region in both CD44v9-positive and CD44v9-negative cells in endoscopically resected early gastric cancer tissue from a patient at 40 months after *H. pylori* eradication (72-year-old male, well-differentiated adenocarcinoma), with written informed consent (Figure S5D). In addition to performing a general pathological assessment, LC3B and CD44v9 were stained using fluorescent immunohistochemistry for a paraffin-embedded pathological tissue specimen. In cells expressing CD44v9, there were fewer LC3B-positive puncta than in CD44v9-negative cells, suggesting that autophagy was repressed within the CD44v9-positive cells (Figure 7F). These results indicate that the accumulation of intracellular CagA with autophagy inhibition was confirmed in CD44v9-expressing cancer stem-like cells of human gastric adenocarcinoma.

## DISCUSSION

The present study reveals that the accumulation of intracellular CagA in CD44v9-expressing cancer stem-like cells is caused by the repression of autophagy. The autophagic pathway associated with CagA degradation is induced as follows: m1VacA-induced GSH deficiency via binding to LRP1 and then enhances Akt phosphorylation at Ser473. Activation of Akt induces MDM2-mediated p53 degradation through the ubiquitin-proteasome system and then activates autophagy.

Figures S1I and S3D indicated that binding of m1VacA to LRP1 was required for the reduction of intracellular GSH levels and the induction of autophagy, causing CagA degradation. In contrast,

(C) AGS cells infected with *H. pylori* (s1m1VacA) for 5 hr were incubated in a medium containing antibiotic for the indicated times with 250 μM acetovanillone (NOX inhibitor), 20 μM MnTMPyP (MnSOD mimic), or 10 mM NAC. p53 expression and LC3-II formation were examined. Data represent the mean ± SD of three independent assays; *p < 0.05, **p < 0.01, compared to AGS cells at 0 hr after eradication (p53-expression, middle panel). None indicates without inhibitor.
(D) AGS cells infected with *H. pylori* (s1m1VacA) for 5 hr were incubated in a medium containing antibiotic for the indicated times with 250 μM acetovanillone (NOX inhibitor), 20 μM MnTMPyP (MnSOD mimic), or 10 mM NAC, and intracellular CagA levels were examined. Data represent the mean ± SD of three independent assays; **p < 0.01. None indicates without inhibitor.
(E) AGS cells infected with *H. pylori* (s1m1VacA) for 5 hr were incubated in a medium containing antibiotic for 15 and 24 hr, and intracellular GSH levels were measured. Data represent the mean ± SD of three independent assays; **p < 0.01.
(F) AGS cells or CagA-expressing WT-A10 cells were incubated with m1VacA for 24 hr, and intracellular GSH levels were measured. Data represent the mean ± SD of three independent assays; **p < 0.01. See also Figure S3.

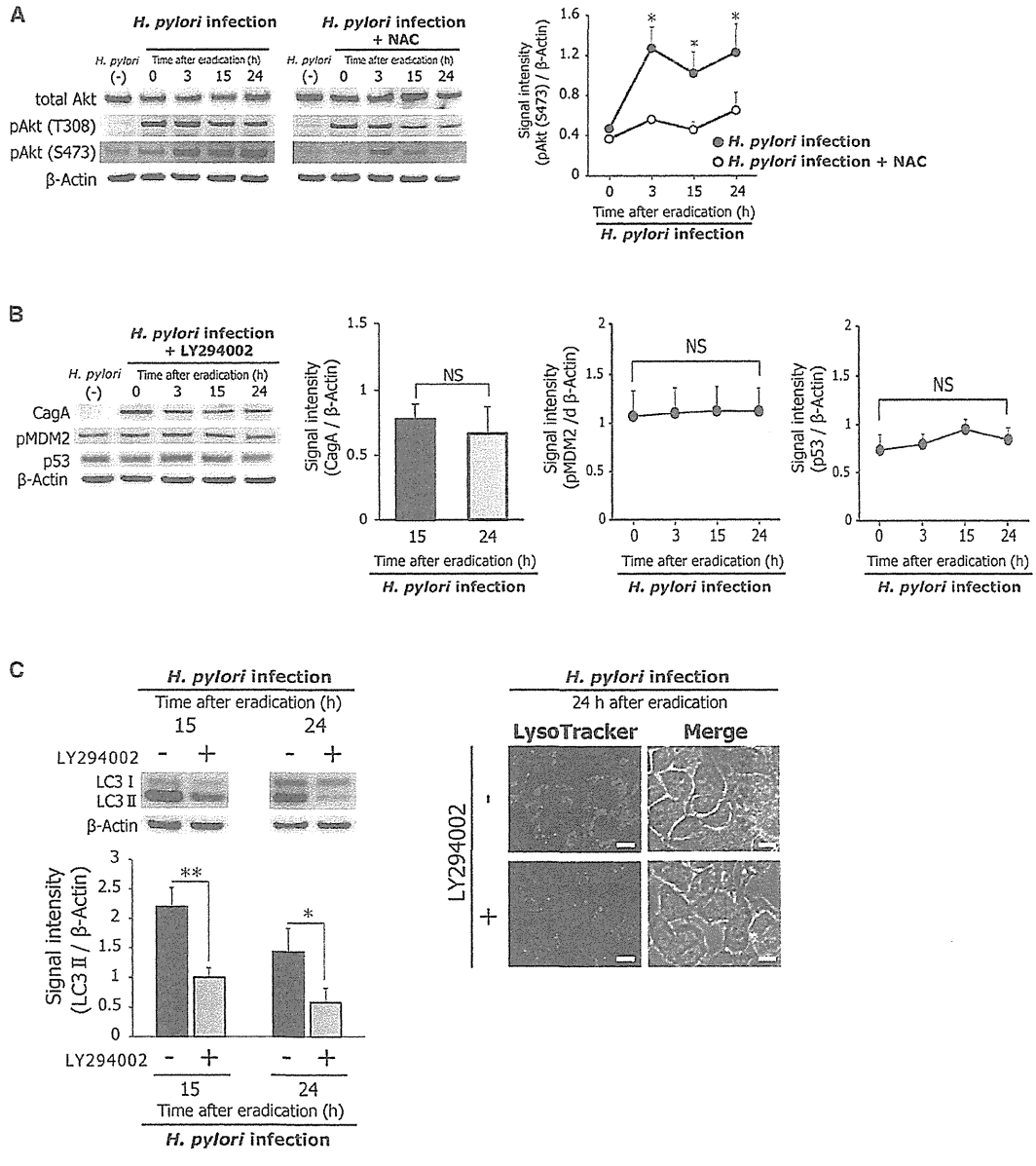


**Figure 6. Akt Phosphorylation in Response to Intracellular ROS Accumulation Contributes to Induction of Autophagy, Causing CagA Degradation**

(A) AGS cells infected with *H. pylori* for 5 hr were incubated in a medium containing antibiotic for the indicated times, with or without 10 mM NAC. Akt phosphorylation at Thr308 and Ser473 was examined. Data represent the mean ± SD of three independent assays; *p < 0.05, compared to AGS cells at 0 hr after eradication (right panel).

(B) AGS cells infected with *H. pylori* for 5 hr were incubated in a medium containing antibiotic for the indicated time with 10 μM LY294002 (Akt-phosphorylation inhibitor), and the levels of intracellular CagA, pMDM, and p53 were examined. Data represent the mean ± SD of three independent assays; NS, not significant.

(C) AGS cells infected with *H. pylori* for 5 hr were incubated in a medium containing antibiotic for the indicated times with 10 μM LY294002 (Akt-phosphorylation inhibitor), and LC3-II formation was examined. Data represent the mean ± SD of three independent assays; *p < 0.05, **p < 0.01. AGS cells at 24 hr after eradication with or without LY294002 were stained using LysoTracker Red DND-99 (right panel). Scale bar = 50 μm. See also Figure S4.

the binding to LRP1 of m2VacA was not detectable by immunoprecipitation assay (Figure S1I). It has been reported that the mid-region of VacA has an important role in the binding of VacA to host cells (Cover and Blanke, 2005). Therefore, these findings suggest that the reason m2VacA could not induce autophagy was the lack of binding ability to LRP1, unlike m1VacA.

Our observations indicate that m1VacA reduces intracellular CagA levels via the induction of autophagy (Figure 3). Intracellular CagA deregulates SHP-2 and PAR1, which promote cell

proliferation, thus causing loss of cell polarity (Saito et al., 2010). Therefore, an excess of intracellular CagA leads to cell damage that disturbs the attachment of bacteria to gastric epithelial cells. Recently, it was suggested that VacA can downregulate CagA-induced signal-transduction in gastric epithelial cells to some extent, thus minimizing the degree of cellular damage (Yokoyama et al., 2005). Therefore, this CagA degradation response to VacA is considered an important strategy for the long-term colonization of the gastric mucosa by *H. pylori*.

*H. pylori* ATCC700392-derived CagA contains the EPIYA-ABC motif, and CagA expressed in WT-A10 cells contains the EPIYA-ABCCC motif derived from *H. pylori* NCTC11637. Our data showed that both of these types of CagA were degraded by autophagy induced by m1VacA (Figures 1, 2, and 3). These results suggest that CagA degradation by autophagy is not affected by differences in the EPIYA motif.

A number of studies demonstrated a link between CagA and gastric cancer development (Blaser et al., 1995; Huang et al., 2003). However, intracellular CagA was only detected in the gastric mucosa of *H. pylori*-infected patients with atrophic gastritis, and not in the gastric mucosa of patients with intestinal metaplasia or cancer (Yamazaki et al., 2003). Therefore, CagA was thought to play a causative role at a relatively early phase of gastric carcinogenesis. Our findings indicate that intracellular CagA is degraded by autophagy induced by the accumulation of intracellular ROS. Thus, even if CagA is translocated into a host cell, it does not persist for a long period. The accumulation of intracellular CagA is restricted to cells in which autophagy is suppressed. We demonstrated that intracellular CagA specifically accumulates in CD44v9-expressing human gastric cancer cells in which CagA degradation by autophagy has been suppressed by their resistance to ROS (Figure 7E). Thus, we show a direct molecular link between CagA and gastric cancer stem-like cells and suggest that the role of CagA in gastric carcinogenesis is not restricted to the early phase.

Chronic inflammation triggers the expression of CD44s (Ishimoto et al., 2010), suggesting that chronic severe inflammation after long-term *H. pylori* colonization induces CD44 expression in normal gastric epithelial cells. CD44-expressing cells have increased intracellular GSH levels, as compared to CD44-negative cells, by maintaining PPP flux and the consequent production of NADPH (Tamada et al., 2012) (Figure S5B), suggesting that CD44-positive cells are slightly resistant to oxidative stress. Conversely, CD44v9-expressing cells are more resistant to oxidative stress, compared with CD44s-expressing cells, by enhancing intracellular GSH levels through the promotion of xCT-mediated cystine uptake (Ishimoto et al., 2011) (Figure S5B). Thus, CagA specifically accumulates in CD44v9-expressing cells by escaping from the autophagy induced by ROS (Figure 7). Additionally, the mRNA expression of *lgr5*, one of the markers of stem cells besides CD44, was not detectable in the CD44- or CD44v9-expressing MKN28 cells (data not shown). Takaishi et al. (2009) reported that the expression of other potential cell-surface markers did not show any correlation with CD44-expressing gastric cancer stem cells. From these findings, we conclude that the accumulation of intracellular CagA by inhibition of autophagy is a specific character of CD44v9-expressing gastric cancer stem-like cells because of their resistance of ROS, and it does not correlate with LGR5. A variety of CD44 isoforms are generated by alternative splicing of the pre-mRNA. CD44v9 is one of the CD44 isoforms and is expressed in gastric cancer stem cells (Mayer et al., 1993). In addition, *H. pylori* infection induced CD44v9 expression, suggesting that the development of cells that accumulate CagA can be caused by *H. pylori* infection (Fan et al., 1996). CD44v9 expression, which is regulated by epithelial splicing regulatory protein 1, plays a functional role in carcinogenesis, differentiation, and metastasis (Yae et al., 2012). In addition, CagA oncogenic signals were maintained in CD44v9-expressing cancer stem-like cells in the present study.

xCT, stabilized by CD44v9, plays an important role in maintaining intracellular redox balance (Patel et al., 2004). Sulfasalazine, a potent xCT inhibitor that has been used routinely for the treatment of inflammatory bowel disease and rheumatoid arthritis, suppresses metastasis of CD44v9-expressing lung cancer and inhibits hepatocellular carcinoma cell growth (Yae et al., 2012). In the present study, sulfasalazine also inhibited the accumulation of intracellular CagA in CD44v9-expressing cells by suppressing autophagy (Figure 7D), suggesting a prophylactic effect for sulfasalazine against CagA-dependent gastric cancer development, especially by targeting cancer stemness.

## EXPERIMENTAL PROCEDURES

### In Vitro *H. pylori* Infection Model

Cells were incubated with s1m1VacA *H. pylori*, VacA-negative *H. pylori*, s1m2VacA *H. pylori*, and s2m2VacA *H. pylori* for 5 hr (multiplicity of infection of 50), and the cells were incubated with RPMI1640 culture medium containing 400 μg/ml kanamycin to kill extracellular bacteria with or without each inhibitor (MG132, Lact, 3MA, Wort, LY294002, nutlin-3, or sulfasalazine) or each antioxidant (acetovanillone, MnTMPyP, or NAC) for the indicated incubation period (0, 3, 15, and 24 hr). The cells were then washed three times with PBS and harvested.

### Preparation of *H. pylori* Culture Supernatants

s1m1VacA, VacA-negative, s1m2VacA, and s2m2VacA *H. pylori*, normalized to an $OD_{600}$ of 0.3, were transferred to cell culture medium (RPMI1640 medium supplemented with 10% FBS) and cultured for a further 15 hr. The supernatants were collected by centrifugation, passed through 0.22 μm filter units to remove any bacteria, and diluted with fresh medium.

### Immunohistochemistry

Tissue was fixed in 4% paraformaldehyde, embedded in paraffin, and sectioned at a thickness of 4 μm. The sections were depleted of paraffin and then rehydrated in a graded series of ethanol solutions. For immunohistochemistry, the sections were washed in Tris-buffered saline with Tween-20 (TBS-T) and subjected to antigen retrieval by heating for 10 min at 105°C in Target Retrieval Solution (pH 9.0) (Dako, Tokyo). Nonspecific binding was blocked by Protein Block (Dako). The sections were incubated overnight at 4°C with primary antibody (see Supplemental Experimental Procedures). Immunoreactivity was detected using Alexa Fluor 568-conjugated goat anti-mouse IgG (Invitrogen, Carlsbad, CA), Alexa Fluor 568-conjugated goat anti-rabbit IgG (Invitrogen), and Alexa Fluor 488-conjugated goat anti-rat IgG (Invitrogen). The samples were examined using an FV10i fluorescence microscope (Olympus, Tokyo).

### Electron Immunocytochemistry

CagA-expressing WT-A10 cells stimulated with 100 nM rapamycin for 24 hr were fixed with 4% paraformaldehyde and 0.1% glutaraldehyde for 80 min. The specimens were then dehydrated in a graded ethanol series and processed with a postembedding immunocytochemical technique using reduced osmium and acrylate resin. Immunogold labeling was performed by incubation with an anti-CagA goat polyclonal antibody (bK-300, 1:1000, Santa Cruz Biotechnology), followed by the addition of secondary antibodies conjugated

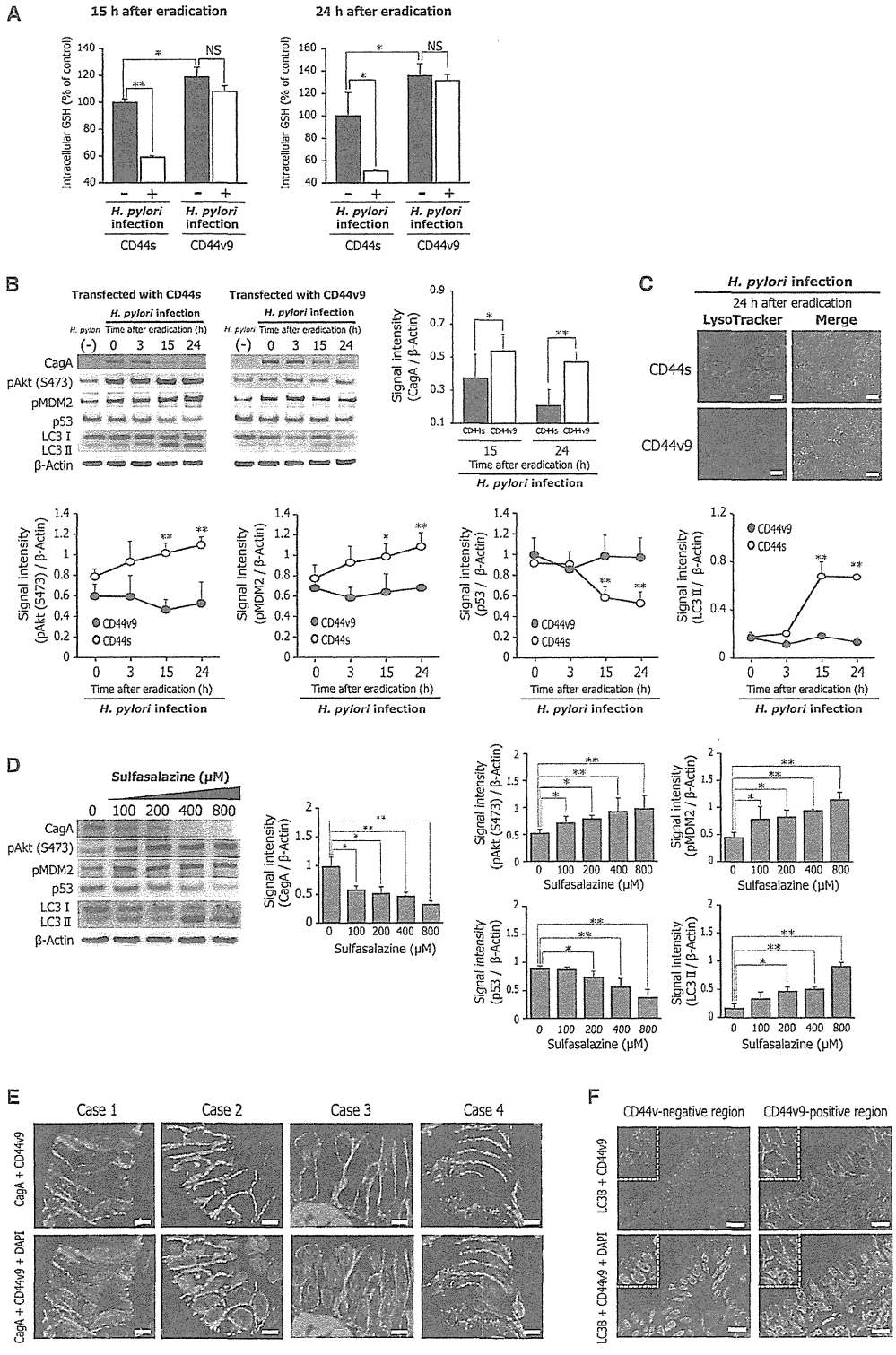


**Figure 7. Accumulation of Intracellular CagA Is Detected in CD44v9-Expressing Gastric Cancer Stem-like Cells**

(A) MKN28 cells were transfected with the pRC/CMV-CD44s or pRC/CMV-CD44v expression plasmid; cells infected with *H. pylori* (s1m1VacA) for 5 hr were incubated in a medium containing antibiotic for 15 and 24 hr, and intracellular GSH levels were examined. Data represent the mean ± SD of three independent assays; *p < 0.05, **p < 0.01; NS, not significant.

to 15 nm gold particles. The sections were poststained with uranyl acetate and modified Sato's lead solution and visualized using a JEM-1200EX electron microscope (JEOL, Tokyo).

### Cell Vacuolation Assay

CagA expression in WT-A10 cells was induced by treatment with m1VacA or m2VacA for 24 hr, and the extent of vacuolation was determined quantitatively by measuring the uptake of neutral red.

### Immunoprecipitation Assay

After s1m1VacA and s1m2VacA *H. pylori* infection for 5 hr, the cell lysates were incubated overnight with anti-LRP1 monoclonal antibody (Santa Cruz Biotechnology) at 4°C. This was followed by the addition of EZview Red Protein A Affinity Gel (Sigma) and overnight incubation. Proteins were detected using antibodies against VacA (Yahiro et al., 1999).

### Fluorescence Immunocytochemistry

To detect EGFP-LC3B signals, AGS cells transfected with the EGFP-LC3B plasmid were infected with *H. pylori* for 5 hr. The cells were incubated with RPMI1640 culture medium containing 400 μg/ml kanamycin—with or without an autophagy inhibitor (3MA and Wort)—for 24 hr, fixed with 4% paraformaldehyde, and incubated with the anti-CagA antibody (AUSTRAL Biologicals). Alexa Fluor 568-conjugated goat anti-mouse IgG (Invitrogen) was used as the secondary antibody. To detect the LysoTracker signals, after *H. pylori* infection for 5 hr, the AGS cells were incubated with RPMI1640 culture medium containing 400 μg/ml kanamycin for 24 hr, and then with LysoTracker Red DND-99 (Invitrogen) for 90 min, followed by fixation with 4% paraformaldehyde. The samples were examined using an FV10i fluorescence microscope (Olympus).

### Measurement of ROS

After *H. pylori* infection for 5 hr, AGS cells were incubated in RPMI1640 culture medium containing 400 μg/ml kanamycin for 15 or 24 hr. The cells were incubated with 10 μM CM-$H_2$DCFDA (Invitrogen) in Hanks balanced salt solution (HBSS) for 60 min at 37°C and washed three times with PBS. To label mitochondria, the cells were incubated with 10 μM MitoTracker Red FM (Invitrogen) in HBSS for 30 min. The samples were examined using an FV10i fluorescence microscope (Olympus). To quantify the intensity of DCF fluorescence, the cells were dissociated using 1 mM EDTA and subjected to flow cytometry using a Gallios Flow Cytometer (Beckman Coulter, Brea, CA) and analysis software (Summit V6.0.2.11185) (Beckman Coulter).

### GSH Assay

Intracellular GSH levels were determined using a GSH-Glo Glutathione Assay Kit (Promega, Madison, WI). The cells ($2 \times 10^3$ per well) were plated in 96-well plates. This assay is based on the conversion of a luciferin derivative to luciferin by glutathione S-transferase in the presence of GSH. The signal generated in a coupled reaction with firefly luciferase is proportional to the amount of GSH in the sample. The assay results were normalized using the GSH standard solution provided with the kit.

### Western Blotting

Total protein (10 μg/lane) was separated on a 4%–12% NuPAGE gradient gel (Invitrogen) and transferred to a PVDF membrane (Invitrogen), which was probed with each primary antibody, followed by reprobing with an anti-actin antibody (Sigma) as the loading control. Signal detection of the immunoreactive bands was facilitated by enhanced chemiluminescence using ECL plus (GE Healthcare, Piscataway, NJ). Signal quantification was performed using the ImageJ program (National Institutes of Health).

### Statistical Analysis

All values are expressed as means ± SD. The statistical significance of differences between two groups was evaluated using Student's t test. Analysis was performed using JSTAT statistical software (version 8.2). Statistical significance was accepted at $p < 0.05$, unless otherwise indicated.

### Tissue Specimens

Human gastric adenocarcinoma tissue specimens were obtained from a 62-year-old female (case 1), a 68-year-old male (case 2), a 72-year-old male (case 3), a 78-year-old male (case 4), an 80-year-old female (*H. pylori*-negative patient), and a 72-year-old male (patient at 40 months after *H. pylori* eradication) who underwent endoscopic submucosal dissection at Keio University Hospital after receiving written informed consent before the procedure. Pathological diagnosis was well-differentiated adenocarcinoma according to the Japanese Gastric Cancer Association classification of gastric carcinoma (14th edition). The study protocol was approved by the ethics committees of Keio University School of Medicine and registered with the UMIN Clinical Trials Registry (UMIN000001057; http://www.umin.ac.jp/ctr/). The study was performed in accordance with the principles of the Declaration of Helsinki.

## SUPPLEMENTAL INFORMATION

Supplemental Information includes five figures and Supplemental Experimental Procedures and can be found with this article online at http://dx.doi.org/10.1016/j.chom.2012.10.014.

## ACKNOWLEDGMENTS

The authors are grateful to Misa Kanekawa for providing general technical assistance and to Hiroshi Takase (Hanaichi Ultrastructure Research Institute) for technical assistance with electron immunocytochemistry. This work was supported by a Grant-in-Aid for Young Scientists (B) (23790156, to H.T.) and a Grant-in-Aid for Scientific Research (B) (22300169 to H.Suzuki) from the Japan Society for the Promotion of Science (JSPS), a grant from the Smoking Research Foundation (to H.Suzuki), and the Keio Gijuku Academic Development Fund (to H.Suzuki).

Received: July 20, 2012
Revised: September 22, 2012
Accepted: October 11, 2012
Published: December 12, 2012

(B) MKN28 cells were transfected with the pRC/CMV-CD44s or pRC/CMV-CD44v expression plasmid; cells infected with *H. pylori* (s1m1VacA) for 5 hr were incubated in a medium containing antibiotic for the indicated times, and intracellular CagA levels were quantified. Data represent the mean ± SD of three independent assays; *$p < 0.05$, **$p < 0.01$. Akt and MDM2 phosphorylation, p53 expression, and LC3-II formation were quantified. Data represent the mean ± SD of three independent assays; *$p < 0.05$, **$p < 0.01$, compared to each cell at 0 hr after eradication.

(C) Representative staining for LysoTracker Red DND-99 is shown. MKN28 cells were transfected with the pRC/CMV-CD44s or pRC/CMV-CD44v expression plasmid; cells infected with *H. pylori* (s1m1VacA) for 5 hr were incubated in a medium containing antibiotic for the indicated times, and the cells were stained using LysoTracker Red DND-99. Scale bar = 50 μm.

(D) MKN28 cells were transfected with the pRC/CMV-CD44v expression plasmid; cells infected with *H. pylori* ATCC700392 (s1m1VacA) for 5 hr were incubated in a medium containing antibiotic with sulfasalazine for 24 hr; and intracellular CagA, pAkt (Ser473), pMDM2, p53, and LC3-II formation were examined. Data represent the mean ± SD of three independent assays; *$p < 0.05$, **$p < 0.01$.

(E) Immunostaining of CagA and CD44v9 in human gastric adenocarcinoma. Case 1, Case 2, Case 3, and Case 4 indicate each gastric adenocarcinoma tissue specimen from the four different patients. Red staining indicates intracellular CagA and green indicates CD44v9. Nuclei (blue) were stained with DAPI. Scale bar = 20 μm.

(F) Immunostaining of LC3 and CD44v9 in human gastric adenocarcinoma. The left panel indicates a CD44v9-negative region and the right panel indicates a CD44v9-positive region. Red staining indicates LC3B-positive puncta and green indicates CD44v9. Nuclei (blue) were stained with DAPI. Scale bar = 30 μm. See also Figure S5.

## REFERENCES

Atkuri, K.R., Mantovani, J.J., Herzenberg, L.A., and Herzenberg, L.A. (2007). N-Acetylcysteine—a safe antidote for cysteine/glutathione deficiency. Curr. Opin. Pharmacol. *7*, 355–359.

Basso, D., Zambon, C.F., Letley, D.P., Stranges, A., Marchet, A., Rhead, J.L., Schiavon, S., Guariso, G., Ceroti, M., Nitti, D., et al. (2008). Clinical relevance of Helicobacter pylori cagA and vacA gene polymorphisms. Gastroenterology *135*, 91–99.

Blaser, M.J., Perez-Perez, G.I., Kleanthous, H., Cover, T.L., Peek, R.M., Chyou, P.H., Stemmermann, G.N., and Nomura, A. (1995). Infection with Helicobacter pylori strains possessing cagA is associated with an increased risk of developing adenocarcinoma of the stomach. Cancer Res. *55*, 2111–2115.

Cover, T.L., and Blanke, S.R. (2005). Helicobacter pylori VacA, a paradigm for toxin multifunctionality. Nat. Rev. Microbiol. *3*, 320–332.

Dalerba, P., Dylla, S.J., Park, I.K., Liu, R., Wang, X., Cho, R.W., Hoey, T., Gurney, A., Huang, E.H., Simeone, D.M., et al. (2007). Phenotypic characterization of human colorectal cancer stem cells. Proc. Natl. Acad. Sci. USA *104*, 10158–10163.

Deretic, V., and Levine, B. (2009). Autophagy, immunity, and microbial adaptations. Cell Host Microbe *5*, 527–549.

Ding, S.Z., Minohara, Y., Fan, X.J., Wang, J., Reyes, V.E., Patel, J., Dirden-Kramer, B., Boldogh, I., Ernst, P.B., and Crowe, S.E. (2007). Helicobacter pylori infection induces oxidative stress and programmed cell death in human gastric epithelial cells. Infect. Immun. *75*, 4030–4039.

Dong-Yun, S., Yu-Ru, D., Shan-Lin, L., Ya-Dong, Z., and Lian, W. (2003). Redox stress regulates cell proliferation and apoptosis of human hepatoma through Akt protein phosphorylation. FEBS Lett. *542*, 60–64.

Fan, X., Long, A., Goggins, M., Fan, X., Keeling, P.W., and Kelleher, D. (1996). Expression of CD44 and its variants on gastric epithelial cells of patients with Helicobacter pylori colonisation. Gut *38*, 507–512.

Hatakeyama, M. (2004). Oncogenic mechanisms of the Helicobacter pylori CagA protein. Nat. Rev. Cancer *4*, 688–694.

Huang, J.Q., Zheng, G.F., Sumanac, K., Irvine, E.J., and Hunt, R.H. (2003). Meta-analysis of the relationship between cagA seropositivity and gastric cancer. Gastroenterology *125*, 1636–1644.

Huang, J., Canadien, V., Lam, G.Y., Steinberg, B.E., Dinauer, M.C., Magalhaes, M.A., Glogauer, M., Grinstein, S., and Brumell, J.H. (2009). Activation of antibacterial autophagy by NADPH oxidases. Proc. Natl. Acad. Sci. USA *106*, 6226–6231.

Ishikawa, S., Ohta, T., and Hatakeyama, M. (2009). Stability of Helicobacter pylori CagA oncoprotein in human gastric epithelial cells. FEBS Lett. *583*, 2414–2418.

Ishimoto, T., Oshima, H., Oshima, M., Kai, K., Torii, R., Masuko, T., Baba, H., Saya, H., and Nagano, O. (2010). CD44+ slow-cycling tumor cell expansion is triggered by cooperative actions of Wnt and prostaglandin E2 in gastric tumorigenesis. Cancer Sci. *101*, 673–678.

Ishimoto, T., Nagano, O., Yae, T., Tamada, M., Motohara, T., Oshima, H., Oshima, M., Ikeda, T., Asaba, R., Yagi, H., et al. (2011). CD44 variant regulates redox status in cancer cells by stabilizing the xCT subunit of system xc(-) and thereby promotes tumor growth. Cancer Cell *19*, 387–400.

Marshall, D.G., Hynes, S.O., Coleman, D.C., O'Morain, C.A., Smyth, C.J., and Moran, A.P. (1999). Lack of a relationship between Lewis antigen expression and cagA, CagA, vacA and VacA status of Irish Helicobacter pylori isolates. FEMS Immunol. Med. Microbiol. *24*, 79–90.

Mayer, B., Jauch, K.W., Günthert, U., Figdor, C.G., Schildberg, F.W., Funke, I., and Johnson, J.P. (1993). De-novo expression of CD44 and survival in gastric cancer. Lancet *342*, 1019–1022.

Miehlke, S., Kirsch, C., Agha-Amiri, K., Günther, T., Lehn, N., Malfertheiner, P., Stolte, M., Ehninger, G., and Bayerdörffer, E. (2000). The Helicobacter pylori vacA s1, m1 genotype and cagA is associated with gastric carcinoma in Germany. Int. J. Cancer *87*, 322–327.

Ogawara, Y., Kishishita, S., Obata, T., Isazawa, Y., Suzuki, T., Tanaka, K., Masuyama, N., and Gotoh, Y. (2002). Akt enhances Mdm2-mediated ubiquitination and degradation of p53. J. Biol. Chem. *277*, 21843–21850.

Ohnishi, N., Yuasa, H., Tanaka, S., Sawa, H., Miura, M., Matsui, A., Higashi, H., Musashi, M., Iwabuchi, K., Suzuki, M., et al. (2008). Transgenic expression of Helicobacter pylori CagA induces gastrointestinal and hematopoietic neoplasms in mouse. Proc. Natl. Acad. Sci. USA *105*, 1003–1008.

Patel, S.A., Warren, B.A., Rhoderick, J.F., and Bridges, R.J. (2004). Differentiation of substrate and non-substrate inhibitors of transport system xc(-): an obligate exchanger of L-glutamate and L-cystine. Neuropharmacology *46*, 273–284.

Raju, D., Hussey, S., Ang, M., Terebiznik, M.R., Sibony, M., Galindo-Mata, E., Gupta, V., Blanke, S.R., Delgado, A., Romero-Gallo, J., et al. (2012). Vacuolating cytotoxin and variants in Atg16L1 that disrupt autophagy promote Helicobacter pylori infection in humans. Gastroenterology *142*, 1160–1171.

Saito, Y., Murata-Kamiya, N., Hirayama, T., Ohba, Y., and Hatakeyama, M. (2010). Conversion of Helicobacter pylori CagA from senescence inducer to oncogenic driver through polarity-dependent regulation of p21. J. Exp. Med. *207*, 2157–2174.

Scherz-Shouval, R., and Elazar, Z. (2007). ROS, mitochondria and the regulation of autophagy. Trends Cell Biol. *17*, 422–427.

Suzuki, H., Suematsu, M., Ishii, H., Kato, S., Miki, H., Mori, M., Ishimura, Y., Nishino, T., and Tsuchiya, M. (1994). Prostaglandin E1 abrogates early reductive stress and zone-specific paradoxical oxidative injury in hypoperfused rat liver. J. Clin. Invest. *93*, 155–164.

Suzuki, H., Iwasaki, E., and Hibi, T. (2009). Helicobacter pylori and gastric cancer. Gastric Cancer *12*, 79–87.

Takaishi, S., Okumura, T., Tu, S., Wang, S.S., Shibata, W., Vigneshwaran, R., Gordon, S.A., Shimada, Y., and Wang, T.C. (2009). Identification of gastric cancer stem cells using the cell surface marker CD44. Stem Cells *27*, 1006–1020.

Tamada, M., Nagano, O., Tateyama, S., Ohmura, M., Yae, T., Ishimoto, T., Sugihara, E., Onishi, N., Yamamoto, T., Yanagawa, H., et al. (2012). Modulation of glucose metabolism by CD44 contributes to antioxidant status and drug resistance in cancer cells. Cancer Res. *72*, 1438–1448.

Terebiznik, M.R., Raju, D., Vázquez, C.L., Torbricki, K., Kulkarni, R., Blanke, S.R., Yoshimori, T., Colombo, M.I., and Jones, N.L. (2009). Effect of Helicobacter pylori's vacuolating cytotoxin on the autophagy pathway in gastric epithelial cells. Autophagy *5*, 370–379.

Uemura, N., Okamoto, S., Yamamoto, S., Matsumura, N., Yamaguchi, S., Yamakido, M., Taniyama, K., Sasaki, N., and Schlemper, R.J. (2001). Helicobacter pylori infection and the development of gastric cancer. N. Engl. J. Med. *345*, 784–789.

Wang, H.J., Kuo, C.H., Yeh, A.A., Chang, P.C., and Wang, W.C. (1998). Vacuolating toxin production in clinical isolates of Helicobacter pylori with different vacA genotypes. J. Infect. Dis. *178*, 207–212.

Wei, J., Nagy, T.A., Vilgelm, A., Zaika, E., Ogden, S.R., Romero-Gallo, J., Piazuelo, M.B., Correa, P., Washington, M.K., El-Rifai, W., et al. (2010). Regulation of p53 tumor suppressor by Helicobacter pylori in gastric epithelial cells. Gastroenterology *139*, 1333–1343.

Yae, T., Tsuchihashi, K., Ishimoto, T., Motohara, T., Yoshikawa, M., Yoshida, G.J., Wada, T., Masuko, T., Mogushi, K., Tanaka, H., et al. (2012). Alternative splicing of CD44 mRNA by ESRP1 enhances lung colonization of metastatic cancer cell. Nat Commun. *3*, 883.

Yahiro, K., Niidome, T., Kimura, M., Hatakeyama, T., Aoyagi, H., Kurazono, H., Imagawa, K., Wada, A., Moss, J., and Hirayama, T. (1999). Activation of Helicobacter pylori VacA toxin by alkaline or acid conditions increases its binding to a 250-kDa receptor protein-tyrosine phosphatase beta. J. Biol. Chem. *274*, 36693–36699.

Yahiro, K., Satoh, M., Nakano, M., Hisatsune, J., Isomoto, H., Sap, J., Suzuki, H., Nomura, F., Noda, M., Moss, J., and Hirayama, T. (2012). Low-density lipoprotein receptor-related protein-1 (LRP1) mediates autophagy and apoptosis caused by Helicobacter pylori VacA. J. Biol. Chem. *287*, 31104–31115.

Yamaoka, Y., Kodama, T., Kita, M., Imanishi, J., Kashima, K., and Graham, D.Y. (1998). Relationship of vacA genotypes of Helicobacter pylori to cagA status, cytotoxin production, and clinical outcome. Helicobacter *3*, 241–253.

Yamazaki, S., Yamakawa, A., Ito, Y., Ohtani, M., Higashi, H., Hatakeyama, M., and Azuma, T. (2003). The CagA protein of Helicobacter pylori is translocated into epithelial cells and binds to SHP-2 in human gastric mucosa. J. Infect. Dis. *187*, 334–337.

Yokoyama, K., Higashi, H., Ishikawa, S., Fujii, Y., Kondo, S., Kato, H., Azuma, T., Wada, A., Hirayama, T., Aburatani, H., and Hatakeyama, M. (2005). Functional antagonism between Helicobacter pylori CagA and vacuolating toxin VacA in control of the NFAT signaling pathway in gastric epithelial cells. Proc. Natl. Acad. Sci. USA *102*, 9661–9666.

Zhou, B.P., Liao, Y., Xia, W., Zou, Y., Spohn, B., and Hung, M.C. (2001). HER-2/neu induces p53 ubiquitination via Akt-mediated MDM2 phosphorylation. Nat. Cell Biol. *3*, 973–982.

Oncogene (2013), 1–8

www.nature.com/onc

REVIEW

# Redox regulation in stem-like cancer cells by CD44 variant isoforms

O Nagano[1], S Okazaki[1] and H Saya[1,2]

Increasing evidence indicates that several types of solid tumor are hierarchically organized and sustained by a distinct population of cancer stem cells (CSCs). CSCs possess enhanced mechanisms of protection from stress induced by reactive oxygen species (ROS) that render them resistant to chemo- and radiotherapy. Expression of CD44, especially variant isoforms (CD44v) of this major CSC marker, contributes to ROS defense through upregulation of the synthesis of reduced glutathione (GSH), the primary intracellular antioxidant. CD44v interacts with and stabilizes xCT, a subunit of the cystine-glutamate transporter xc(-), and thereby promotes cystine uptake for GSH synthesis. Given that cancer cells are often exposed to high levels of ROS during tumor progression, the ability to avoid the consequences of such exposure is required for cancer cell survival and propagation *in vivo*. CSCs, in which defense against ROS is enhanced by CD44v are thus thought to drive tumor growth, chemoresistance and metastasis. Therapy targeted to the CD44v-xCT system may therefore impair the ROS defense ability of CSCs and thereby sensitize them to currently available treatments.

*Oncogene* advance online publication, 21 January 2013; doi:10.1038/onc.2012.638

**Keywords:** cancer stem cell; CD44; reactive oxygen species; cystine-glutamate transporter

## INTRODUCTION

Tumor formation, relapse, and metastasis are thought to be driven by cancer stem cells (CSCs), a subpopulation of cancer cells that give rise to a hierarchical organization of tumors.[1,2] CSCs are selectively capable of self-renewal and tumor initiation, and they generate the bulk population of nontumorigenic cells in a tumor through differentiation. Given that cancer cells are exposed to environmental stressors such as oxygen or nutrient deficiency, low pH, inflammatory mediators and reactive oxygen species (ROS) *in vivo*,[3,4] the ability to avoid the consequences of such exposure is required for the maintenance of CSCs. Furthermore, the efficacy of cancer therapies including radiation therapy and anticancer drugs is attributable in part to the production of ROS and the consequent induction of oxidative stress in cancer cells.[5] CSCs are generally more resistant to oxidative stress provoked by chemo- or radiotherapy compared with non-stem-like cancer cells, however.[6–8] The targeting of antioxidant systems in CSCs that possess the ability to avoid the adverse consequences of oxidative stress might therefore be expected to improve the efficacy of cancer treatment. This review summarizes current knowledge of the role of variant (v) isoforms of CD44 in redox regulation in cancer cells and in resistance to cancer therapy.

### The CSC marker CD44 and its variant isoforms

The most widely expressed cell surface markers of CSCs in solid tumors are CD133, CD24, CD44, CD166, CD29 and EpCAM (CD326), with CD44 being the most prevalent of these CSC markers.[9–11] CD44 is thus highly expressed in CSCs derived from solid tumors including breast,[12] prostate,[13] colon,[14] head and neck[15] and pancreatic[16] cancer.

CD44 is a single-pass type I transmembrane protein and functions as a cellular adhesion molecule for hyaluronic acid, a major component of the extracellular matrix.[17–19] It exists in numerous isoforms that are generated through alternative splicing of CD44 precursor mRNA.[19] Epithelial splicing regulatory protein 1 (ESRP1) and ESRP2 were recently shown to have a key role in the inclusion of variant exons in the mature forms of CD44 mRNA.[20] Whereas the standard isoform of CD44 (CD44s) is expressed predominantly in hematopoietic cells and normal epithelial cell subsets, CD44v isoforms, which contain additional insertions in the membrane-proximal extracellular region, are highly expressed in epithelial-type carcinomas. Expression of CD44v in some tissues appears to relate to tumor progression, in particular to the metastatic potential of some cancers.[21–24]

Although the functional relevance of CD44 expression in CSCs remains to be established,[11] CD44 is thought to be associated with features of CSCs that are shared with normal stem or progenitor cells, such as interaction with the corresponding niche,[25,26] the potential for cell migration and homing,[27–29] the capacity for defense against ROS[30,31] and resistance to apoptosis.[32–34] Indeed, RNA interference–mediated depletion of CD44 has revealed that CD44 expression influences the stem-like properties of CSC populations isolated from human breast,[35] prostate[36] and colon[37,38] cancers, suggesting that CD44 is a potential target for CSC-directed therapy.

Genetic ablation of CD44 in a colon cancer model, the *Apc*$^{Min}$ mouse, was shown to attenuate the formation of aberrant crypts, implicating CD44 in tumorigenesis.[39] In contrast, genetic ablation of CD44 in a breast cancer model (MMTV-PyVmT mouse)[40] or a gastric cancer model (*K19-Wnt1/C2mE* mouse)[30] did not reduce the incidence of tumor formation, suggesting that CD44 is not

[1]Division of Gene Regulation, Institute for Advanced Medical Research, School of Medicine, Keio University, Shinjuku-ku, Tokyo, Japan and [2]Japan Science and Technology Agency, Core Research for Evolutional Science and Technology (CREST), K's Gobancho, Chiyoda-ku, Tokyo, Japan. Correspondence: Dr O Nagano, Division of Gene Regulation, Institute for Advanced Medical Research, School of Medicine, Keio University, 35 Shinanomachi, Shinjuku-ku, Tokyo 160-8582, Japan.
E-mail: osmna@sb3.so-net.ne.jp
Received 2 October 2012; revised 2 December 2012; accepted 3 December 2012

required for onset of tumor formation in these mice. The CD44 dependence of tumor initiation might thus be determined by cellular context.

Although few studies have focused on the role of CD44v in CSCs, it was recently reported that colorectal CSCs express CD44v and that the induction of CD44v expression in these cells was associated with activation of the proto-oncoprotein MET, implicating CD44v in regulation of signaling by MET and its ligand, hepatocyte growth factor.[37] Given that MET promotes the invasive growth of both stem cells and cancer cells,[41] such CD44v-mediated MET activation might also enhance the invasive growth potential of CSCs.

## Promotion of the mesenchymal phenotype by CD44s

The epithelial-mesenchymal transition (EMT) is characterized by the loss of epithelial characteristics and the gain of mesenchymal attributes and is a key event in wound healing, tissue repair and several diseases in adults.[42,43] During the EMT, epithelial cells downregulate cell-cell adhesion systems, lose their polarity, and acquire a mesenchymal phenotype associated with increased interaction with the extracellular matrix as well as an enhanced migratory capacity.[44] Induction of the EMT in several epithelial-type cells was recently found to be accompanied by a shift in CD44 isoforms from CD44v to CD44s that occurs concomitantly with downregulation of ESRP expression.[45–47] Of note, CD44s has been shown to promote the EMT through the activation of signaling by transforming growth factor β[48,49] and the protein kinase AKT.[45] Furthermore, CD44s interacts with its major ligand (hyaluronic acid) more effectively than do CD44v isoforms.[50,51] Together, these observations implicate CD44s, but not CD44v, in the acquisition of mesenchymal properties, including enhanced extracellular matrix interaction and transforming growth factor β signaling, by cancer cells.

## Regulation of CD44v by the EMT and hypoxia in cancer cells

CD44v is thus highly expressed in epithelial-type carcinomas, and induction of the EMT is associated with a shift in CD44 isoforms from CD44v to CD44s. Experimental induction of the EMT might therefore be expected to elicit an isoform shift from CD44v to CD44s in epithelial cell lines. However, CD44v expression does not always appear to conform to EMT status in cancer cells. We recently found that the expression of CD44 isoforms is not associated with that of EMT markers in 4T1 metastatic mouse breast cancer cells, which include both $CD44v^+$ cells (which predominantly express CD44v) and $CD44v^-$ cells (which express only CD44s).[52] Furthermore, chromatin immunoprecipitation–sequencing (ChIP-seq) analysis at the *ESRP1* gene locus revealed the presence of histone H3 trimethylated at $Lys^4$ (H3K4me3), a mark of active transcription, at the transcription start site in $CD44v^+$ cells but the presence of H3K27me3, a mark of transcriptional repression, at this site in $CD44v^-$ cells,[52] suggesting that CD44v expression is regulated by histone modification at the ESRP1 locus rather than by EMT status in 4T1 cells. Together, these findings suggest that CD44v is not a specific marker for epithelial cancer cells and CD44s is not a specific marker for mesenchymal cancer cells.

Tumor hypoxia has emerged as an important factor in the induction of a pathological EMT leading to cancer progression.[53–55] Hypoxia and hypoxia-inducible factor-1α were recently shown to stimulate CD44v expression in MDA-MB-231 and SUM-149 breast cancer cells,[56] which exhibit a mesenchymal phenotype.[57] CD44v expression in cancer cells could be thus regulated by EMT independent mechanism. Furthermore, hypoxia signaling promotes the attachment of sialyl Lewis X glycan to CD44v, but not to CD44s, and the modifed CD44v may serve as a ligand for E-selectin expressed in endothelial cells during cancer metastasis.[58,59] The generation of such glycan-modified CD44v concomitant with the EMT might thus have a role in the promotion of cancer progression by tumor hypoxia.

## Modulation of the activity of cell surface proteins by CD44v

An emerging concept in signal transduction is that CD44 functions as a co-receptor.[19] A complex of CD44s and a phosphorylated ERM (ezrin/radixin/moesin) protein initiates activation of the transforming growth factor β receptor and the downstream SMAD signaling complex, thereby contributing to acquisition of the mesenchymal phenotype.[49] In addition, several variant-specific domains of CD44 isoforms interact with other cell surface proteins at the plasma membrane (Figure 1). The CD44v3 isoform, (which includes the sequence encoded by variant exon 3) undergoes heparin sulfate modification and interacts with various growth factors, including heparin-binding epidermal growth factor–like growth factor and basic fibroblast growth factor.[60] Furthermore, such interaction of the pro form of heparin-binding epidermal growth factor–like growth factor with CD44v3 promotes its cleavage by matrix metalloproteinase 7,

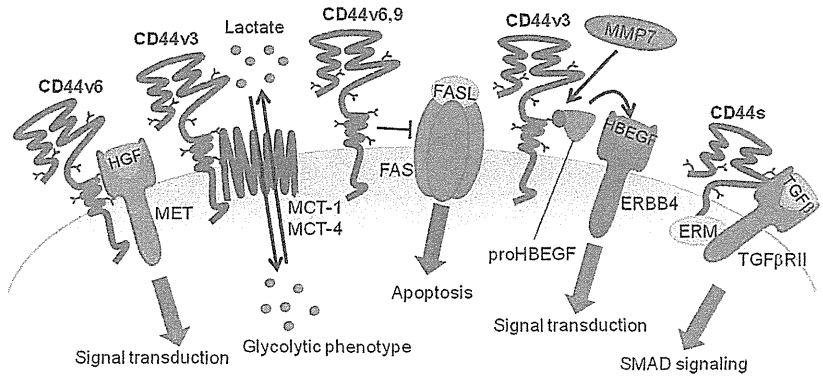


**Figure 1.** Regulation of cell surface proteins by CD44. A complex of CD44s and a phosphorylated ERM (ezrin/radixin/moesin) protein initiates activation of the TGFβ receptor (TGFβRII) and the downstream SMAD signaling complex, thereby contributing to acquisition of the mesenchymal phenotype. The CD44v3 isoform interacts with the pro form of heparin-binding epidermal growth factor–like growth factor and thereby promotes its conversion to the active form by MMP7. CD44v6 acts as a co-receptor of the receptor tyrosine kinase MET and thereby promotes signaling by HGF. CD44v3 also interacts with monocarboxylate transporter-1 and monocarboxylate transporter-4, which are responsible for lactate transport, and may thereby contribute to the glycolytic phenotype of cancer cells. CD44v6 and CD44v9 interact with FAS and inhibit programmed cell death induced by FAS ligand (FASL).

yielding the active form of the growth factor that binds to and activates signaling by the receptor tyrosine kinase ERBB4.[61] The CD44v3-mediated activation of heparin-binding epidermal growth factor–like growth factor and its presentation to ERBB4 may therefore contribute to the efficient activation of ERBB4 signaling. The CD44v6 isoform has been shown to act as a co-receptor of the receptor tyrosine kinase MET.[62] CD44v3 also interacts with monocarboxylate transporter-1 and monocarboxylate transporter-4, both of which are responsible for the transport of lactate in breast cancer cells.[63] On the other hand, CD44v6 and CD44v9 interact with the death receptor FAS (CD95) in lipid rafts and thereby interfere with death receptor signaling and inhibit apoptosis.[32] CD44v isoforms may thus serve to modulate the functions of various plasma membrane proteins, including receptor tyrosine kinases, transporters, and a death receptor in cancer cells rather than as mediators of extracellular matrix interaction, with the latter function being subserved primarily by CD44s.

## The importance of redox regulation in CSCs

Moderate levels of ROS stimulate cell proliferation, whereas high levels that overwhelm the cellular antioxidant capacity trigger cell death. Increased levels of ROS also promote aging of hematopoietic stem cells,[64,65] whereas high ROS levels in *Drosophila* sensitize hematopoietic progenitors to the induction of differentiation.[66] The accumulation of ROS in stem cells may thus reduce their self-renewal capability through the activation of aging- or differentiation-related signaling pathways, such as those mediated by $p16^{INK4a}$ and the retinoblastoma protein[67,68] or by p38 mitogen-activated protein kinase.[64,69] Both CSCs of breast cancer and normal mammary stem cells possess an enhanced ROS defense capability compared with their non-stem cell counterparts.[7,8] Strategies to abrogate ROS defense in CSCs might thus be expected to result in the eradication of these ROS-resistant cells and thereby to provide a basis for the development of efficient cancer therapies.

It is also possible that CSCs are located in a hypoxic microenvironment and therefore show resistance to chemo- or radiotherapy,[6,70] the cytotoxicity of which requires the availability of local oxygen.[71] A more thorough understanding of the CSC niche and elucidation of the mechanisms underlying redox regulation in CSCs may thus lead to improved therapeutic approaches for cancer.

## Major sources of ROS in cancer

Mitochondrial respiration is a major source of ROS in most mammalian cells.[72,73] However, most cancer cells metabolize glucose predominantly via aerobic glycolysis and therefore might not rely on mitochondrial respiration for energy production.[74] In such cancer cells, generation of ROS likely results both from increased metabolic activities due to aberrant growth factor and cytokine signaling and to oncogene activation[75–77] as well as from increased activity of ROS-producing enzymes such as NADPH oxidase, cyclooxygenases and lipoxygenases.[77,78] In the tumor microenvironment, ROS also can be derived from extrinsic sources. Tumor-infiltrating inflammatory cells such as macrophages and neutrophils generate ROS as a result of NADPH oxidase activation.[78,79]

Cancer therapies including chemo- and radiation therapy also induce ROS generation.[5] Indeed, the mechanism of action of radiotherapy relies primarily on the production of ROS.[71,80] Given that radiation induces mitotic cell death in dividing cells,[81,82] most proliferative tumor cells are more sensitive to radiotherapy than quiescent normal cells. Anticancer drugs, including the anthracyclines and platinum coordination complexes, also exert their anticancer effects as well as toxic side effects through ROS generation.[83]

Cancer cells that are often exposed to high levels of ROS derived from intrinsic or extrinsic sources thus likely require a well-organized antioxidant defense system for their survival *in vivo* (Figure 2).

## Redox adaptation in cancer cells

Oxidative stress occurs when the production of ROS exceeds the capacity of the cellular defense system, which consists of redox enzymes and other antioxidant molecules. Oncogenic cell proliferation is coupled to the generation of ROS,[68,84] and cancer cells have therefore evolved mechanisms to protect themselves from oxidative stress and have developed adaptation strategies, including the upregulation of both antioxidants and prosurvival molecules.[5] One consequence of such redox adaptation is that ROS-inducing cancer therapies alone may not be sufficient to damage CSCs, in which the upregulation of antioxidant capacity is especially pronounced.

The adaptation mechanisms include upregulation of redox-sensitive transcription factors, elevation of ROS-scavenging capacity and altered regulation of redox-sensitive death or survival factors. Reduced glutathione (GSH), a ubiquitous reducing thiol peptide that serves as an important intracellular redox buffer, also have a role in redox adaptation in cancer cells. Biosynthesis of GSH is catalyzed by two sequential enzymatic reactions (Figure 3).[85–87] First, glutamate-cysteine ligase, which consists of catalytic glutamate-cysteine ligase and modifier glutamate-cysteine ligase subunits, catalyzes the formation of γ-glutamylcysteine from glutamate and cysteine. Glutathione synthetase then couples glycine to γ-glutamylcysteine to form GSH. Tumor cells manifest elevated levels of both GSH and GSH metabolic enzymes, which confer resistance to cancer therapies.[88,89] Natural compounds such as β-phenylethyl isothiocyanate and pipelongumine have recently been shown to influence GSH metabolism and to selectively kill transformed cells without affecting normal cells.[90,91] The targeting of GSH metabolism may thus effectively disable redox adaptation by cancer cells and thereby damage those cells with active metabolism that leads to the production of high levels of ROS.

## The cystine-glutamate antiporter system xc(-)

System xc(-) is composed of a light-chain subunit (xCT or SLC7A11) and a heavy-chain subunit (CD98hc or SLC3A2) and functions as a $Na^+$-independent transporter that mediates the exchange of extracellular cystine (the predominant form of cysteine in plasma, extracellular body fluids and cell culture medium) for intracellular glutamate.[92–94] The availability of cysteine is rate limiting for GSH synthesis,[95] with the activity of system xc(-) therefore being essential for the GSH-dependent antioxidant system. Mice lacking xCT appear healthy, but they have an increased plasma concentration of cystine compared with their wild-type littermates,[94] suggesting that xCT-mediated cystine transport may be required for cells exposed to severe oxidative stress. Indeed, transcription of the xCT gene is induced by oxidative stress due to electrophilic agents, depletion of cystine, or oxygen, with this effect being mediated through the binding of the transcription factor Nrf2 to its response element in the promoter of the xCT gene.[96] Furthermore, activating transcription factor 4, which has a key role in the response of cells to multiple types of stress,[97] has been shown to upregulate xCT expression.[98,99] These various observations thus indicate that xCT contributes to the protection of cells exposed to high levels of ROS.

xCT interacts with the type II transmembrane protein CD98hc at the cell surface.[100] Indeed, CD98hc is separately and covalently linked to several light chains that function as amino acid transporters at the plasma membrane, including LAT1, LAT2, y+LAT1, y+LAT2, ASC-1 and xCT.[101] The precise mechanism by which CD98hc selects its binding partner to give rise to the

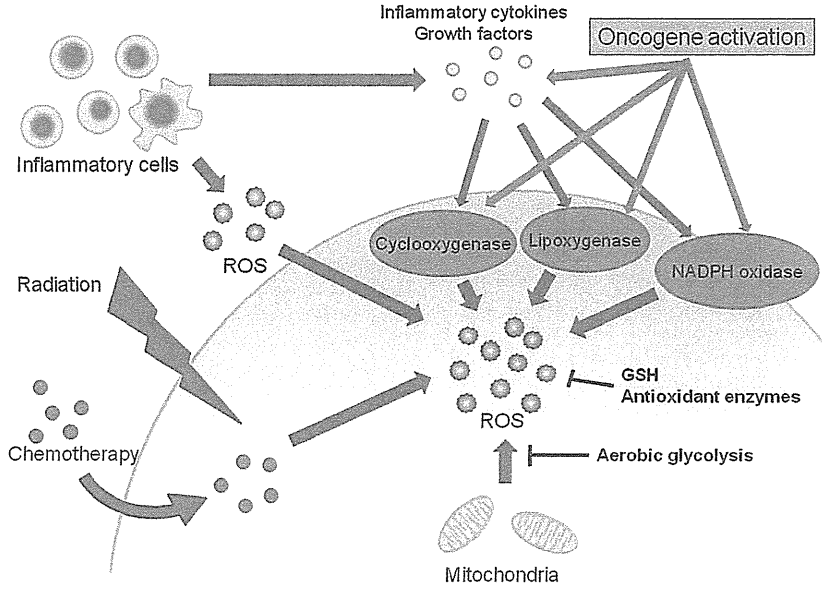


**Figure 2.** Major sources of ROS in cancer. Most cancer cells metabolize glucose predominantly via aerobic glycolysis and therefore might not rely on mitochondrial respiration, which results in ROS production. In such cancer cells, generation of ROS likely results both from increased metabolic activities due to aberrant growth factor and cytokine signaling and to oncogene activation as well as from increased activity of ROS-producing enzymes such as NADPH oxidase, cyclooxygenases and lipoxygenases. In the tumor microenvironment, tumor-infiltrating inflammatory cells such as macrophages and neutrophils release ROS as well as inflammatory cytokines. Cancer therapies including chemo- and radiation therapy also induce ROS generation.

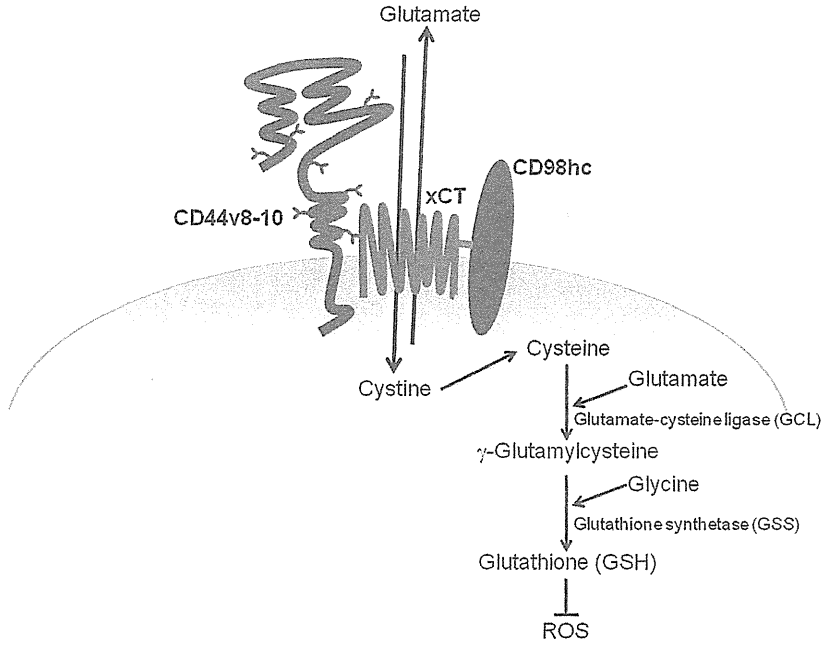


**Figure 3.** Stabilization of xCT and promotion of cystine uptake by CD44v. CD44v contributes to ROS defense by promoting the synthesis of GSH, a primary intracellular antioxidant. CD44v interacts with and stabilizes xCT, a subunit of the cystine-glutamate transporter xc(-), and thereby promotes the uptake of cystine for GSH synthesis. Glutamate-cysteine ligase catalyzes the formation of γ-glutamylcysteine from glutamate and cysteine, and glutathione synthetase then couples glycine to γ-glutamylcysteine to form GSH.

different types of functional amino acid transporter has remained unclear, however.

Stabilization of xCT and promotion of cystine uptake by CD44v

Expression of xCT at the surface of cancer cells was found to be modulated by CD44v8-10 (an isoform that includes the sequence encoded by variant exons 8 – 10), which interacts with and thereby stabilizes xCT at the plasma membrane, resulting in promotion of GSH synthesis[30] (Figure 3). RNAi-mediated ablation of CD44v thus reduced the cell surface expression of xCT and thereby depleted intracellular cysteine without affecting the intracellular content of other amino acids. CD44v thus has a key role in the GSH-dependent antioxidant system in cancer cells

through modulation of xCT-mediated cystine transport and consequent GSH synthesis.

The monitoring of xc(-) transporter activity by positron emission tomography with an $^{18}$F-labeled glutamate derivative was recently shown to be beneficial for the detection of tumors in patients with non-small cell lung cancer or breast cancer.[102] The maximum standardized uptake value for the tracer was found to be significantly correlated with the intensity of immunohistochemical staining for xCT and CD44 in tumor specimens. Although the expression of CD44v specifically was not examined in this study, highly CD44-expressing cancer cells might thus depend on the xc(-) transporter for their survival and propagation in human tumors.

## The role of CD44v-xCT in cancer metastasis

Cancer metastasis is now thought to result from the dissemination of stem-like cancer cells and their colonization of tissue distant from the primary tumor site.[103–105] Among human breast cancer cell lines, CD44-positive cells with a high level of aldehyde dehydrogenase activity ($ALDH^{high}CD44^{+}$ cells) show increased tumor formation and lung colonization abilities compared with $ALDH^{low}CD44^{low/-}$ cells.[106] CD44-expressing cancer cells isolated from lung metastases in a mouse xenograft model of human breast cancer were also recently found to be highly enriched in tumor-initiating cells.[107] Among prostate cancer cells, $CD44^{+}$ stem-like cells have been shown to possess metastatic activity,[108] and forced expression of mir-34a in such cells (in which the abundance of this microRNA is reduced compared with that in CD44-negative cells) was found to inhibit metastasis through suppression of CD44 expression.[36] Together, these observations suggest that $CD44^{+}$ stem-like cancer cells have an important role in cancer metastasis.

CD44 and its variant isoforms have been implicated in multiple steps required for cancer metastasis, including matrix invasion, extravasation and colonization.[11,18,29,109] Genetic ablation of CD44 in a mouse model of metastatic osteosarcoma ($Trp53^{+/tm1}$ mouse) did not affect the incidence of primary tumor formation, but it did abrogate metastasis, implicating CD44 in metastasis rather than in tumor initiation in this model.[110] On the other hand, genetic ablation of CD44 in the MMTV-PyVmT mouse model of breast cancer enhanced metastatic activity.[40] Furthermore, forced expression of the microRNAs miR-373 and miR-520c, which suppress CD44 expression, was found to confer metastatic activity on *MCF-7* breast cancer cells, which normally show a nonmigratory and nonmetastatic phenotype.[111] These observations indicate that CD44 suppresses invasion and metastasis in these breast cancer cells. The dependence of metastasis on CD44 expression thus also seems to be dependent on the cellular context, as appears to be the case for tumor-initiating ability in CSCs. Alternatively, the shift in specific splicing isoform expression rather than a change in baseline CD44 transcription may be associated with those biologic characteristics of CSCs.

In cancer metastasis, the disseminating cells are often exposed to various environmental stressors including ROS. The ability to avoid the consequences of such exposure is therefore required for metastatic CSCs to successfully colonize secondary sites. The redox protein thioredoxin-like 2 was recently shown to regulate the growth and metastasis of human breast cancer cells. Knockdown of redox protein thioredoxin-like 2 in human breast cancer cell lines thus increased ROS levels and thereby reduced the activity of the transcription factor NF-κB, resulting in inhibition of tumor formation and lung metastasis.[112] These results thus also suggested that metastatic growth requires adequate ROS defense ability. Neutrophils were also recently shown to accumulate in the lungs before the arrival of metastatic cells as well as to inhibit lung metastasis of mouse 4T1 metastatic breast cancer cells through NADPH-dependent generation of $H_2O_2$.[113] In the 4T1 mouse model, we recently found that CD44v-expressing lung metastases contain high levels of GSH, but not of its oxidized form glutathione disulfide (glutathione-S-S-glutathione, GSSG), and that CD44v expression enhanced xCT-dependent ROS defense and thereby allowed cancer cells to evade metastatic stress and to colonize the lung.[52] In a mouse model of melanoma metastasis based on B16 melanoma cells, enhanced synthesis of GSH was found to contribute to resistance to oxidative stress and thereby to promote metastatic growth in the liver.[114,115] Collectively, these observations suggest that neutralization of oxidative stress through the action of the GSH-dependent antioxidant system or other redox proteins at potential sites of metastasis may be required for CSCs to establish metastatic lesions (Figure 4).

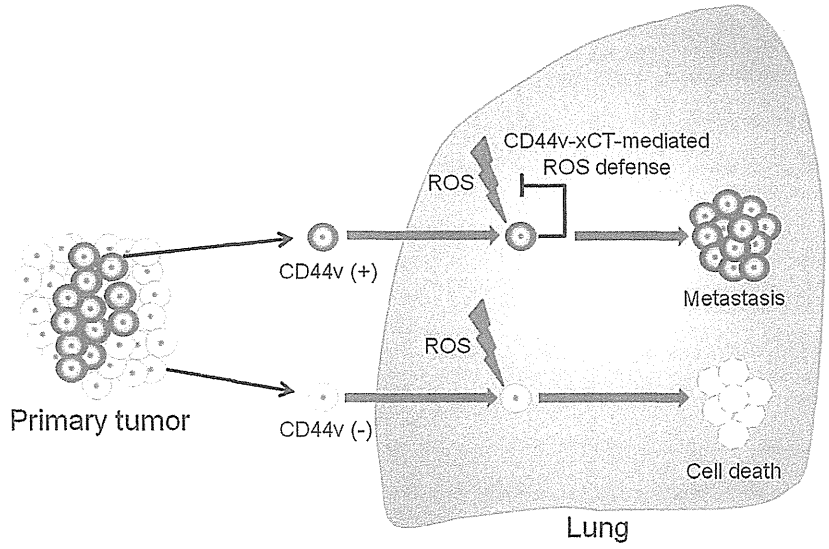


**Figure 4.** The role of CD44v-xCT in cancer metastasis. ESRP-regulated alternative splicing of CD44 mRNA results in CD44v expression in metastatic CSCs. CD44v-expressing cancer cells possess an increased ability to defend against ROS as a result of enhanced xCT-mediated cystine uptake and consequent GSH synthesis. Such cells with a high level of GSH are thus predominantly responsible for colonization of the lung, a tissue that contains high levels of ROS ($H_2O_2$) produced by inflammatory cells such as neutrophils.

Perspective

Conventional cancer therapies result in a transient reduction in tumor mass through the killing of non-stem cancer cells. Frequently, however, the cancer reemerges after a few months or even years as a result of the failure to eliminate CSCs. Furthermore, the formation of metastases is thought to result from the dissemination of CSC-like cells and their colonization of secondary sites. Future improvements in cancer treatment may thus require the development of drugs that target signaling or metabolic pathways that are activated specifically in CSC-like cells rather than in non-stem cancer cells, the latter of which are sensitive to currently available treatments.

Redox adaptation by cancer cells contributes to their survival under conditions of persistent oxidative stress due to their intrinsic active metabolism and extrinsic factors in the tumor microenvironment, and it results in resistance to certain anticancer agents. In CSCs, such redox adaptation may be potentiated as a result of their enhanced antioxidant capacity. The targeting of redox regulation in CSCs is thus a candidate approach to CSC-directed therapy. The identification of the main pool of antioxidants that maintains redox status in each type of CSC might lead to the development of efficient therapies for treatment-resistant cancers. In CD44v-expressing CSCs, xCT-dependent cystine transport and consequent synthesis of GSH appear to enhance ROS defense and contribute to redox adaptation. Therapy targeted to the CD44v-xCT system may therefore impair ROS defense ability as well as redox adaptation in CSCs and thereby sensitize them to currently available treatments.

## CONFLICT OF INTEREST

The authors declare no conflict of interest.

## ACKNOWLEDGEMENTS

We thank K Arai for help in preparation of the manuscript. The work in the authors' laboratory was supported by grants from the Ministry of Education, Culture, Sports, Science, and Technology of Japan (to HS) as well as by the Ministry's Project for Development of Innovative Research on Cancer Therapeutics (P-Direct, to ON).

## REFERENCES

1 Clevers H. The cancer stem cell: premises, promises and challenges. *Nat Med* 2011; **17**: 313–319.
2 Visvader JE, Lindeman GJ. Cancer stem cells in solid tumours: accumulating evidence and unresolved questions. *Nat Rev Cancer* 2008; **8**: 755–768.
3 Chiang AC, Massague J. Molecular basis of metastasis. *N Engl J Med* 2008; **359**: 2814–2823.
4 Gupta GP, Massague J. Cancer metastasis: building a framework. *Cell* 2006; **127**: 679–695.
5 Trachootham D, Alexandre J, Huang P. Targeting cancer cells by ROS-mediated mechanisms: a radical therapeutic approach? *Nat Rev Drug Discov* 2009; **8**: 579–591.
6 Baumann M, Krause M, Hill R. Exploring the role of cancer stem cells in radioresistance. *Nat Rev Cancer* 2008; **8**: 545–554.
7 Diehn M, Cho RW, Lobo NA, Kalisky T, Dorie MJ, Kulp AN *et al.* Association of reactive oxygen species levels and radioresistance in cancer stem cells. *Nature* 2009; **458**: 780–783.
8 Phillips TM, McBride WH, Pajonk F. The response of $CD24^{(-/low)}/CD44^{+}$ breast cancer-initiating cells to radiation. *J Natl Cancer Inst* 2006; **98**: 1777–1785.
9 Ailles LE, Weissman IL. Cancer stem cells in solid tumors. *Curr Opin Biotechnol* 2007; **18**: 460–466.
10 Lobo NA, Shimono Y, Qian D, Clarke MF. The biology of cancer stem cells. *Annu Rev Cell Dev Biol* 2007; **23**: 675–699.
11 Zoller M. CD44: Can a cancer-initiating cell profit from an abundantly expressed molecule? *Nat Rev Cancer* 2011; **11**: 254–267.
12 Al-Hajj M, Wicha MS, Benito-Hernandez A, Morrison SJ, Clarke MF. Prospective identification of tumorigenic breast cancer cells. *Proc Natl Acad Sci USA* 2003; **100**: 3983–3988.
13 Collins AT, Berry PA, Hyde C, Stower MJ, Maitland NJ. Prospective identification of tumorigenic prostate cancer stem cells. *Cancer Res* 2005; **65**: 10946–10951.
14 Dalerba P, Dylla SJ, Park IK, Liu R, Wang X, Cho RW *et al.* Phenotypic characterization of human colorectal cancer stem cells. *Proc Natl Acad Sci USA* 2007; **104**: 10158–10163.
15 Prince ME, Sivanandan R, Kaczorowski A, Wolf GT, Kaplan MJ, Dalerba P *et al.* Identification of a subpopulation of cells with cancer stem cell properties in head and neck squamous cell carcinoma. *Proc Natl Acad Sci USA* 2007; **104**: 973–978.
16 Li C, Heidt DG, Dalerba P, Burant CF, Zhang L, Adsay V *et al.* Identification of pancreatic cancer stem cells. *Cancer Res* 2007; **67**: 1030–1037.
17 Aruffo A, Stamenkovic I, Melnick M, Underhill CB, Seed B. CD44 is the principal cell surface receptor for hyaluronate. *Cell* 1990; **61**: 1303–1313.
18 Nagano O, Saya H. Mechanism and biological significance of CD44 cleavage. *Cancer Sci* 2004; **95**: 930–935.
19 Ponta H, Sherman L, Herrlich PA. CD44: from adhesion molecules to signalling regulators. *Nat Rev Mol Cell Biol* 2003; **4**: 33–45.
20 Warzecha CC, Sato TK, Nabet B, Hogenesch JB, Carstens RP. ESRP1 and ESRP2 are epithelial cell-type-specific regulators of FGFR2 splicing. *Mol Cell* 2009; **33**: 591–601.
21 Gunthert U, Hofmann M, Rudy W, Reber S, Zoller M, Haussmann I *et al.* A new variant of glycoprotein CD44 confers metastatic potential to rat carcinoma cells. *Cell* 1991; **65**: 13–24.
22 Reber S, Matzku S, Gunthert U, Ponta H, Herrlich P, Zoller M. Retardation of metastatic tumor growth after immunization with metastasis-specific monoclonal antibodies. *Int J Cancer* 1990; **46**: 919–927.
23 Seiter S, Arch R, Reber S, Komitowski D, Hofmann M, Ponta H *et al.* Prevention of tumor metastasis formation by anti-variant CD44. *J Exp Med* 1993; **177**: 443–455.
24 Tanabe KK, Ellis LM, Saya H. Expression of CD44R1 adhesion molecule in colon carcinomas and metastases. *Lancet* 1993; **341**: 725–726.
25 Jin L, Hope KJ, Zhai Q, Smadja-Joffe F, Dick JE. Targeting of CD44 eradicates human acute myeloid leukemic stem cells. *Nat Med* 2006; **12**: 1167–1174.
26 Preston M, Sherman LS. Neural stem cell niches: roles for the hyaluronan-based extracellular matrix. *Front Biosci* 2011; **3**: 1165–1179.
27 Lapidot T, Dar A, Kollet O. How do stem cells find their way home? *Blood* 2005; **106**: 1901–1910.
28 Sackstein R, Merzaban JS, Cain DW, Dagia NM, Spencer JA, Lin CP *et al. Ex vivo* glycan engineering of CD44 programs human multipotent mesenchymal stromal cell trafficking to bone. *Nat Med* 2008; **14**: 181–187.
29 DeGrendele HC, Estess P, Siegelman MH. Requirement for CD44 in activated T cell extravasation into an inflammatory site. *Science* 1997; **278**: 672–675.
30 Ishimoto T, Nagano O, Yae T, Tamada M, Motohara T, Oshima H *et al.* CD44 variant regulates redox status in cancer cells by stabilizing the xCT subunit of system xc(-) and thereby promotes tumor growth. *Cancer Cell* 2011; **19**: 387–400.
31 Shi X, Zhang Y, Zheng J, Pan J. Reactive oxygen species in cancer stem cells. *Antioxid Redox Signal* 2012; **16**: 1215–1228.
32 Mielgo A, van Driel M, Bloem A, Landmann L, Gunthert U. A novel antiapoptotic mechanism based on interference of Fas signaling by CD44 variant isoforms. *Cell Death Differ* 2006; **13**: 465–477.
33 Bourguignon LY, Earle C, Wong G, Spevak CC, Krueger K. Stem cell marker (Nanog) and Stat-3 signaling promote MicroRNA-21 expression and chemoresistance in hyaluronan/CD44-activated head and neck squamous cell carcinoma cells. *Oncogene* 2012; **31**: 149–160.
34 Toole BP, Slomiany MG. Hyaluronan, CD44 and Emmprin: partners in cancer cell chemoresistance. *Drug Resist Update* 2008; **11**: 110–121.
35 Pham PV, Phan NL, Nguyen NT, Truong NH, Duong TT, Le DV *et al.* Differentiation of breast cancer stem cells by knockdown of CD44: promising differentiation therapy. *J Transl Med* 2011; **9**: 209.
36 Liu C, Kelnar K, Liu B, Chen X, Calhoun-Davis T, Li H *et al.* The microRNA miR-34a inhibits prostate cancer stem cells and metastasis by directly repressing CD44. *Nat Med* 2011; **17**: 211–215.
37 Ohata H, Ishiguro T, Aihara Y, Sato A, Sakai H, Sekine S *et al.* Induction of the stem-like cell regulator CD44 by Rho kinase inhibition contributes to the maintenance of colon cancer-initiating cells. *Cancer Res* 2012; **72**: 5101–5110.
38 Du L, Wang H, He L, Zhang J, Ni B, Wang X *et al.* CD44 is of functional importance for colorectal cancer stem cells. *Clin Cancer Res* 2008; **14**: 6751–6760.
39 Zeilstra J, Joosten SP, Dokter M, Verwiel E, Spaargaren M, Pals ST. Deletion of the WNT target and cancer stem cell marker CD44 in $Apc(_{Min}/+)$ mice attenuates intestinal tumorigenesis. *Cancer Res* 2008; **68**: 3655–3661.
40 Lopez JI, Camenisch TD, Stevens MV, Sands BJ, McDonald J, Schroeder JA. CD44 attenuates metastatic invasion during breast cancer progression. *Cancer Res* 2005; **65**: 6755–6763.
41 Boccaccio C, Comoglio PM. Invasive growth: a MET-driven genetic programme for cancer and stem cells. *Nat Rev Cancer* 2006; **6**: 637–645.
42 Kalluri R, Neilson EG. Epithelial-mesenchymal transition and its implications for fibrosis. *J Clin Invest* 2003; **112**: 1776–1784.
43 Thiery JP, Acloque H, Huang RY, Nieto MA. Epithelial-mesenchymal transitions in development and disease. *Cell* 2009; **139**: 871–890.

44 Kalluri R, Weinberg RA. The basics of epithelial-mesenchymal transition. *J Clin Invest* 2009; **119**: 1420–1428.
45 Brown RL, Reinke LM, Damerow MS, Perez D, Chodosh LA, Yang J *et al.* CD44 splice isoform switching in human and mouse epithelium is essential for epithelial-mesenchymal transition and breast cancer progression. *J Clin Invest* 2011; **121**: 1064–1074.
46 Shapiro IM, Cheng AW, Flytzanis NC, Balsamo M, Condeelis JS, Oktay MH *et al.* An EMT-driven alternative splicing program occurs in human breast cancer and modulates cellular phenotype. *PLoS Genet* 2011; **7**: e1002218.
47 Warzecha CC, Jiang P, Amirikian K, Dittmar KA, Lu H, Shen S *et al.* An ESRP-regulated splicing programme is abrogated during the epithelial-mesenchymal transition. *EMBO J* 2010; **29**: 3286–3300.
48 Mima K, Okabe H, Ishimoto T, Hayashi H, Nakagawa S, Kuroki H *et al.* CD44s regulates the TGF-β-mediated mesenchymal phenotype and is associated with poor prognosis in patients with hepatocellular carcinoma. *Cancer Res* 2012; **72**: 3414–3423.
49 Takahashi E, Nagano O, Ishimoto T, Yae T, Suzuki Y, Shinoda T *et al.* Tumor necrosis factor-α regulates transforming growth factor-β-dependent epithelial-mesenchymal transition by promoting hyaluronan-CD44-moesin interaction. *J Biol Chem* 2010; **285**: 4060–4073.
50 Bartolazzi A, Jackson D, Bennett K, Aruffo A, Dickinson R, Shields J *et al.* Regulation of growth and dissemination of a human lymphoma by CD44 splice variants. *J Cell Sci* 1995; **108**: 1723–1733.
51 Bennett KL, Modrell B, Greenfield B, Bartolazzi A, Stamenkovic I, Peach R *et al.* Regulation of CD44 binding to hyaluronan by glycosylation of variably spliced exons. *J Cell Biol* 1995; **131**: 1623–1633.
52 Yae T, Tsuchihashi K, Ishimoto T, Motohara T, Yoshikawa M, Yoshida GJ *et al.* Alternative splicing of CD44 mRNA by ESRP1 enhances lung colonization of metastatic cancer cell. *Nat Commun* 2012; **3**: 883.
53 Yang MH, Wu MZ, Chiou SH, Chen PM, Chang SY, Liu CJ *et al.* Direct regulation of TWIST by HIF-1α promotes metastasis. *Nat Cell Biol* 2008; **10**: 295–305.
54 Cooke VG, LeBleu VS, Keskin D, Khan Z, O'Connell JT, Teng Y *et al.* Pericyte depletion results in hypoxia-associated epithelial-to-mesenchymal transition and metastasis mediated by Met signaling pathway. *Cancer Cell* 2012; **21**: 66–81.
55 Sun S, Ning X, Zhang Y, Lu Y, Nie Y, Han S *et al.* Hypoxia-inducible factor-1α induces Twist expression in tubular epithelial cells subjected to hypoxia, leading to epithelial-to-mesenchymal transition. *Kidney Int* 2009; **75**: 1278–1287.
56 Krishnamachary B, Penet MF, Nimmagadda S, Mironchik Y, Raman V, Solaiyappan M *et al.* Hypoxia regulates CD44 and its variant isoforms through HIF-1α in triple negative breast cancer. *PLoS One* 2012; **7**: e44078.
57 Neve RM, Chin K, Fridlyand J, Yeh J, Baehner FL, Fevr T *et al.* A collection of breast cancer cell lines for the study of functionally distinct cancer subtypes. *Cancer Cell* 2006; **10**: 515–527.
58 Kannagi R, Sakuma K, Miyazaki K, Lim KT, Yusa A, Yin J *et al.* Altered expression of glycan genes in cancers induced by epigenetic silencing and tumor hypoxia: clues in the ongoing search for new tumor markers. *Cancer Sci* 2010; **101**: 586–593.
59 Hanley WD, Burdick MM, Konstantopoulos K, Sackstein R. CD44 on LS174T colon carcinoma cells possesses E-selectin ligand activity. *Cancer Res* 2005; **65**: 5812–5817.
60 Bennett KL, Jackson DG, Simon JC, Tanczos E, Peach R, Modrell B *et al.* CD44 isoforms containing exon V3 are responsible for the presentation of heparin-binding growth factor. *J Cell Biol* 1995; **128**: 687–698.
61 Yu WH, Woessner Jr JF, McNeish JD, Stamenkovic I. CD44 anchors the assembly of matrilysin/MMP-7 with heparin-binding epidermal growth factor precursor and ErbB4 and regulates female reproductive organ remodeling. *Genes Dev* 2002; **16**: 307–323.
62 Orian-Rousseau V, Chen L, Sleeman JP, Herrlich P, Ponta H. CD44 is required for two consecutive steps in HGF/c-Met signaling. *Genes Dev* 2002; **16**: 3074–3086.
63 Slomiany MG, Grass GD, Robertson AD, Yang XY, Maria BL, Beeson C *et al.* Hyaluronan, CD44, and emmprin regulate lactate efflux and membrane localization of monocarboxylate transporters in human breast carcinoma cells. *Cancer Res* 2009; **69**: 1293–1301.
64 Ito K, Hirao A, Arai F, Takubo K, Matsuoka S, Miyamoto K *et al.* Reactive oxygen species act through p38 MAPK to limit the lifespan of hematopoietic stem cells. *Nat Med* 2006; **12**: 446–451.
65 Tothova Z, Gilliland DG. FoxO transcription factors and stem cell homeostasis: insights from the hematopoietic system. *Cell Stem Cell* 2007; **1**: 140–152.
66 Owusu-Ansah E, Banerjee U. Reactive oxygen species prime *Drosophila* haematopoietic progenitors for differentiation. *Nature* 2009; **461**: 537–541.
67 Macleod KF. The role of the RB tumour suppressor pathway in oxidative stress responses in the haematopoietic system. *Nat Rev Cancer* 2008; **8**: 769–781.
68 Takahashi A, Ohtani N, Yamakoshi K, Iida S, Tahara H, Nakayama K *et al.* Mitogenic signalling and the p16INK4a-Rb pathway cooperate to enforce irreversible cellular senescence. *Nat Cell Biol* 2006; **8**: 1291–1297.
69 Li J, Stouffs M, Serrander L, Banfi B, Bettiol E, Charnay Y *et al.* The NADPH oxidase NOX4 drives cardiac differentiation: role in regulating cardiac transcription factors and MAP kinase activation. *Mol Biol Cell* 2006; **17**: 3978–3988.
70 Keith B, Simon MC. Hypoxia-inducible factors, stem cells, and cancer. *Cell* 2007; **129**: 465–472.
71 Hill RP, Marie-Egyptienne DT, Hedley DW. Cancer stem cells, hypoxia and metastasis. *Semin Radiat Oncol* 2009; **19**: 106–111.
72 Adam-Vizi V, Chinopoulos C. Bioenergetics and the formation of mitochondrial reactive oxygen species. *Trends Pharmacol Sci* 2006; **27**: 639–645.
73 Balaban RS, Nemoto S, Finkel T. Mitochondria, oxidants, and aging. *Cell* 2005; **120**: 483–495.
74 Warburg O. On the origin of cancer cells. *Science* 1956; **123**: 309–314.
75 DeNicola GM, Karreth FA, Humpton TJ, Gopinathan A, Wei C, Frese K *et al.* Oncogene-induced Nrf2 transcription promotes ROS detoxification and tumorigenesis. *Nature* 2011; **475**: 106–109.
76 Dolado I, Swat A, Ajenjo N, De Vita G, Cuadrado A, Nebreda AR. p38α MAP kinase as a sensor of reactive oxygen species in tumorigenesis. *Cancer Cell* 2007; **11**: 191–205.
77 Thannickal VJ, Fanburg BL. Reactive oxygen species in cell signaling. *Am J Physiol Lung Cell Mol Physiol* 2000; **279**: L1005–L1028.
78 Bedard K, Krause KH. The NOX family of ROS-generating NADPH oxidases: physiology and pathophysiology. *Physiol Rev* 2007; **87**: 245–313.
79 Gregory AD, Houghton AM. Tumor-associated neutrophils: new targets for cancer therapy. *Cancer Res* 2011; **71**: 2411–2416.
80 Spitz DR, Azzam EI, Li JJ, Gius D. Metabolic oxidation/reduction reactions and cellular responses to ionizing radiation: a unifying concept in stress response biology. *Cancer Metast Rev* 2004; **23**: 311–322.
81 Golden EB, Pellicciotta I, Demaria S, Barcellos-Hoff MH, Formenti SC. The convergence of radiation and immunogenic cell death signaling pathways. *Front Oncol* 2012; **2**: 88.
82 Hendry JH, West CM. Apoptosis and mitotic cell death: their relative contributions to normal-tissue and tumour radiation response. *Int J Radiat Biol* 1997; **71**: 709–719.
83 Conklin KA. Chemotherapy-associated oxidative stress: impact on chemotherapeutic effectiveness. *Integr Cancer Ther* 2004; **3**: 294–300.
84 Lee AC, Fenster BE, Ito H, Takeda K, Bae NS, Hirai T *et al.* Ras proteins induce senescence by altering the intracellular levels of reactive oxygen species. *J Biol Chem* 1999; **274**: 7936–7940.
85 Arrick BA, Nathan CF. Glutathione metabolism as a determinant of therapeutic efficacy: a review. *Cancer Res* 1984; **44**: 4224–4232.
86 Dalton TP, Chen Y, Schneider SN, Nebert DW, Shertzer HG. Genetically altered mice to evaluate glutathione homeostasis in health and disease. *Free Radic Biol Med* 2004; **37**: 1511–1526.
87 Meister A. Glutathione metabolism and its selective modification. *J Biol Chem* 1988; **263**: 17205–17208.
88 O'Brien ML, Tew KD. Glutathione and related enzymes in multidrug resistance. *Eur J Cancer* 1996; **32A**: 967–978.
89 Tew KD. Glutathione-associated enzymes in anticancer drug resistance. *Cancer Res* 1994; **54**: 4313–4320.
90 Raj L, Ide T, Gurkar AU, Foley M, Schenone M, Li X *et al.* Selective killing of cancer cells by a small molecule targeting the stress response to ROS. *Nature* 2011; **475**: 231–234.
91 Trachootham D, Zhou Y, Zhang H, Demizu Y, Chen Z, Pelicano H *et al.* Selective killing of oncogenically transformed cells through a ROS-mediated mechanism by β-phenylethyl isothiocyanate. *Cancer Cell* 2006; **10**: 241–252.
92 Huang Y, Dai Z, Barbacioru C, Sadee W. Cystine-glutamate transporter SLC7A11 in cancer chemosensitivity and chemoresistance. *Cancer Res* 2005; **65**: 7446–7454.
93 Lo M, Wang YZ, Gout PW. The x(c)- cystine/glutamate antiporter: a potential target for therapy of cancer and other diseases. *J Cell Physiol* 2008; **215**: 593–602.
94 Sato H, Shiiya A, Kimata M, Maebara K, Tamba M, Sakakura Y *et al.* Redox imbalance in cystine/glutamate transporter-deficient mice. *J Biol Chem* 2005; **280**: 37423–37429.
95 Ishii T, Sugita Y, Bannai S. Regulation of glutathione levels in mouse spleen lymphocytes by transport of cysteine. *J Cell Physiol* 1987; **133**: 330–336.
96 Sasaki H, Sato H, Kuriyama-Matsumura K, Sato K, Maebara K, Wang H *et al.* Electrophile response element-mediated induction of the cystine/glutamate exchange transporter gene expression. *J Biol Chem* 2002; **277**: 44765–44771.
97 Harding HP, Zhang Y, Zeng H, Novoa I, Lu PD, Calfon M *et al.* An integrated stress response regulates amino acid metabolism and resistance to oxidative stress. *Mol Cell* 2003; **11**: 619–633.
98 Lewerenz J, Sato H, Albrecht P, Henke N, Noack R, Methner A *et al.* Mutation of ATF4 mediates resistance of neuronal cell lines against oxidative stress by inducing xCT expression. *Cell Death Differ* 2012; **19**: 847–858.

99 Lewerenz J, Maher P. Basal levels of eIF2α phosphorylation determine cellular antioxidant status by regulating ATF4 and xCT expression. *J Biol Chem* 2009; **284**: 1106–1115.
100 Wang H, Tamba M, Kimata M, Sakamoto K, Bannai S, Sato H. Expression of the activity of cystine/glutamate exchange transporter, system x(c)(-), by xCT and rBAT. *Biochem Biophys Res Commun* 2003; **305**: 611–618.
101 Verrey F, Closs EI, Wagner CA, Palacin M, Endou H, Kanai Y. CATs and HATs: the SLC7 family of amino acid transporters. *Pflugers Arch* 2004; **447**: 532–542.
102 Baek S, Choi CM, Ahn SH, Lee JW, Gong G, Ryu JS *et al.* Exploratory clinical trial of (4S)-4-(3-[$^{18}$F]fluoropropyl)-L-glutamate for imaging xC- transporter using positron emission tomography in patients with non-small cell lung or breast cancer. *Clin Cancer Res* 2012; **18**: 5427–5437.
103 Balic M, Lin H, Young L, Hawes D, Giuliano A, McNamara G *et al.* Most early disseminated cancer cells detected in bone marrow of breast cancer patients have a putative breast cancer stem cell phenotype. *Clin Cancer Res* 2006; **12**: 5615–5621.
104 Dieter SM, Ball CR, Hoffmann CM, Nowrouzi A, Herbst F, Zavidij O *et al.* Distinct types of tumor-initiating cells form human colon cancer tumors and metastases. *Cell Stem Cell* 2011; **9**: 357–365.
105 Hermann PC, Huber SL, Herrler T, Aicher A, Ellwart JW, Guba M *et al.* Distinct populations of cancer stem cells determine tumor growth and metastatic activity in human pancreatic cancer. *Cell Stem Cell* 2007; **1**: 313–323.
106 Croker AK, Goodale D, Chu J, Postenka C, Hedley BD, Hess DA *et al.* High aldehyde dehydrogenase and expression of cancer stem cell markers selects for breast cancer cells with enhanced malignant and metastatic ability. *J Cell Mol Med* 2009; **13**: 2236–2252.
107 Liu H, Patel MR, Prescher JA, Patsialou A, Qian D, Lin J *et al.* Cancer stem cells from human breast tumors are involved in spontaneous metastases in orthotopic mouse models. *Proc Natl Acad Sci USA* 2010; **107**: 18115–18120.
108 Patrawala L, Calhoun T, Schneider-Broussard R, Li H, Bhatia B, Tang S *et al.* Highly purified CD44$^+$ prostate cancer cells from xenograft human tumors are enriched in tumorigenic and metastatic progenitor cells. *Oncogene* 2006; **25**: 1696–1708.
109 Naor D, Wallach-Dayan SB, Zahalka MA, Sionov RV. Involvement of CD44, a molecule with a thousand faces, in cancer dissemination. *Semin Cancer Biol* 2008; **18**: 260–267.
110 Weber GF, Bronson RT, Ilagan J, Cantor H, Schmits R, Mak TW. Absence of the CD44 gene prevents sarcoma metastasis. *Cancer Res* 2002; **62**: 2281–2286.
111 Huang Q, Gumireddy K, Schrier M, le Sage C, Nagel R, Nair S *et al.* The microRNAs miR-373 and miR-520c promote tumour invasion and metastasis. *Nat Cell Biol* 2008; **10**: 202–210.
112 Qu Y, Wang J, Ray PS, Guo H, Huang J, Shin-Sim M *et al.* Thioredoxin-like 2 regulates human cancer cell growth and metastasis via redox homeostasis and NF-κB signaling. *J Clin Invest* 2011; **121**: 212–225.
113 Granot Z, Henke E, Comen EA, King TA, Norton L, Benezra R. Tumor entrained neutrophils inhibit seeding in the premetastatic lung. *Cancer Cell* 2011; **20**: 300–314.
114 Anasagasti MJ, Martin JJ, Mendoza L, Obrador E, Estrela JM, McCuskey RS *et al.* Glutathione protects metastatic melanoma cells against oxidative stress in the murine hepatic microvasculature. *Hepatology* 1998; **27**: 1249–1256.
115 Obrador E, Carretero J, Ortega A, Medina I, Rodilla V, Pellicer JA *et al.* γ-Glutamyl transpeptidase overexpression increases metastatic growth of B16 melanoma cells in the mouse liver. *Hepatology* 2002; **35**: 74–81.

THE JOURNAL OF BIOLOGICAL CHEMISTRY VOL. 287, NO. 2, pp. 1397–1405, January 6, 2012


# Competitive Interactions of Cancer Cells and Normal Cells via Secretory MicroRNAs*[S]

Received for publication, August 4, 2011, and in revised form, November 23, 2011 Published, JBC Papers in Press, November 28, 2011, DOI 10.1074/jbc.M111.288662

**Nobuyoshi Kosaka**[‡1], **Haruhisa Iguchi**[‡§1], **Yusuke Yoshioka**[‡2], **Keitaro Hagiwara**[‡¶], **Fumitaka Takeshita**[‡], **and Takahiro Ochiya**[‡3]

*From the* [‡]*Division of Molecular and Cellular Medicine, National Cancer Center Research Institute, 5-1-1, Tsukiji, Chuo-ku, Tokyo 104-0045, Japan,* [§]*Pharmacology Research Laboratories, Dainippon Sumitomo Pharma Co., Ltd., 1-98, Kasugadenaka 3-chome, Konohana-ku, Osaka 554-0022, Japan, and the* [¶]*Department of Biological Information, Graduate School of Bioscience and Biotechnology, Tokyo Institute of Technology, Yokohama, Kanagawa 226-8501, Japan*

**Background:** Homeostatic cell competitive system between cancerous cells and non-cancerous cells is considered as the reason for tumor initiation.
**Results:** Exosomal tumor-suppressive microRNAs secreted by non-cancerous cells inhibit the proliferation of cancerous cells.
**Conclusion:** Exosomal tumor-suppressive microRNAs act as an inhibitory signal for cancer cells in a cell-competitive process.
**Significance:** This provides a novel insight into a tumor initiation mechanism.

**Normal epithelial cells regulate the secretion of autocrine and paracrine factors that prevent aberrant growth of neighboring cells, leading to healthy development and normal metabolism. One reason for tumor initiation is considered to be a failure of this homeostatic cell competitive system. Here we identify tumor-suppressive microRNAs (miRNAs) secreted by normal cells as anti-proliferative signal entities. Culture supernatant of normal epithelial prostate PNT-2 cells attenuated proliferation of PC-3M-luc cells, prostate cancer cells. Global analysis of miRNA expression signature revealed that a variety of tumor-suppressive miRNAs are released from PNT-2 cells. Of these miRNAs, secretory miR-143 could induce growth inhibition exclusively in cancer cells *in vitro* and *in vivo*. These results suggest that secretory tumor-suppressive miRNAs can act as a death signal in a cell competitive process. This study provides a novel insight into a tumor initiation mechanism.**

Competitive interactions among cells are the basis of many homeostatic processes in biology. In *Drosophila*, normal epithelial cells compete with transformed ones for individual survival, which is a process called cell competition (1, 2). If a given group of cells was exposed to some stress, it would be separated into subpopulations of cells with different levels of damage. In noncompetitive conditions, cells with severe damage die in a short time, whereas moderately damaged cells survive to the next generation, indicative of the transduction of a negative phenotype. On the other hand, in competitive conditions even slightly damaged cells are eliminated from the cell group because healthy cells, the "winners," convey death signals to damaged cells, the "losers," and the losers reciprocally confer growth signals to the winners. This feed-forward regulation enables the cell population to eradicate abnormal cells and maintain the same number of normal cells in a limited niche.

Oncogenesis is characterized by genetic and metabolic changes reprogramming living cells to undergo uncontrolled proliferation (3). This suggests that the abnormal cells that are originally destined for elimination can survive and expand against the cell competitive regulation, leading to the formation of a tumor mass. Consistently with this concept, Bondar and Medzhitov (4) showed that the cell competition process involves p53, a tumor-suppressive gene, between the hematopoietic stem cells and progenitor cells, suggesting that gene modifications of p53 could disturb the homeostatic mechanism and give rise to tumor initiation. It is conceivable that p53 target genes could be associated with intercellular communication between winners and losers; however, this literature has not answered the question of whether this regulatory system is mediated by contact-dependent or contact-independent manner. More than 10 years ago a pioneer study suggested that non-cancerous cells co-cultured with cancer cells inhibit the growth of cancer cells *in vitro* (5). This result indicated that humoral factors could be involved in cell competition as intercellular communicators (6).

As recently as a few years ago it was believed that RNAs could not behave as extracellular signal molecules because of their vulnerability to the attack of ribonucleases largely existing in body fluid. Evidence is presently increasing to show that miRNAs[4] contained in exosomes are released from mammalian

* This work was supported in part by a grant-in-aid for the Third-Term Comprehensive 10-Year Strategy for Cancer Control, a grant-in-aid for Scientific Research on Priority Areas Cancer from the Ministry of Education, Culture, Sports, Science, and Technology, the Program for Promotion of Fundamental Studies in Health Sciences of the National Institute of Biomedical Innovation, and the Japan Society for the Promotion of Science through the "Funding Program for World-Leading Innovative R&D on Science and Technology (FIRST Program)" initiated by the Council for Science and Technology Policy.
[S] This article contains supplemental Figs. 1–3.
[1] Both authors contributed equally to this work.
[2] A Research Fellow of the Japan Society for the Promotion of Science.
[3] To whom correspondence should be addressed: Division of Molecular and Cellular Medicine, National Cancer Center Research Institute, 1-1, Tsukiji, 5-chome, Chuo-ku, Tokyo 104-0045, Japan. Tel.: 81-3-3542-2511 (ext. 4800); Fax: 81-3-3541-2685; E-mail: tochiya@ncc.go.jp.

[4] The abbreviations used are: miRNA, microRNA; CM, conditioned medium; luc, luciferase; MTT, 3-(4,5-dimethylthiazol-2-yl)-2,5-diphenyltetrazolium bromide; QRT-PCR, quantitative real time PCR.

cells and act as a signal transducer (7). It is important that many different tumor-suppressive miRNAs, such as miR-16 and miR-143, are down-regulated in cancer cells, resulting in tumorigenesis, tumor progression, and metastasis (8–11). Taken together, these findings suggest that secretory miRNAs may have favorable aspects for anti-proliferative signals mediating cell competition.

In this report we show that miR-143 expression in normal prostate cells, PNT-2 cells, is higher than that in prostate cancer cells, PC-3M-luc cells, and that miR-143 released from non-cancerous cells transfers growth-inhibitory signals to cancerous cells *in vitro* and *in vivo*. These results suggest that secretory tumor-suppressive miRNAs might be a death signal from winners to losers in the context of cell competition. Secretory miRNAs can be conducive to the maintenance of normal growth and development.

## EXPERIMENTAL PROCEDURES

*Reagents*—Mouse monoclonal anti-KRAS (F234) (sc-30) was purchased from Santa Cruz. Rabbit polyclonal anti-ERK5 (#3372) was purchased from Cell Signaling. Mouse monoclonal anti-actin, clone C4 (MAB1501), was obtained from Millipore. Mouse monoclonal ant-human-CD63 antibody (556019) was purchased from BD Pharmingen. Peroxidase-labeled anti-mouse and anti-rabbit antibodies were included in the Amersham Biosciences ECL PLUS Western blotting Reagents Pack (RPN2124) (GE Healthcare). Synthetic *Caenorhabditis elegans* miRNA cel-miR-39 was synthesized by Qiagen (Valencia, CA). Synthetic hsa-miR-143 (pre-miR-143), the negative control 1 (NC1), has-miR-143 inhibitor molecule (anti-miR-143), and the negative control inhibitor molecule (anti-NC) were purchased from Ambion (Austin, TX). GW4869 was purchased from Calbiochem. Geneticin was purchased from Invitrogen.

*Cell Culture*—PNT-2 cells, immortalized normal adult prostatic epithelial cell line, were purchased from the DS Pharma Biomedical Co., Ltd. (Osaka, Japan). HEK293 cells, a human embryonic kidney cell line (CRL-1573), were obtained from American Type Culture Collection (Manassas, VA). HEK293 cells were cultured in Dulbecco's modified Eagle's medium containing 10% heat-inactivated fetal bovine serum (FBS) and an antibiotic-antimycotic (Invitrogen) at 37 °C in 5% $CO_2$. PNT-2 and the prostate cancer cell line, PC-3M-luc cells, continuously expressing firefly luciferase (Xenogen, Alameda, CA), were cultured in RPMI containing 10% heat-inactivated FBS and an antibiotic-antimycotic at 37 °C in 5% $CO_2$.

*Preparation of Conditioned Medium and Exosomes*—Before the collection of culture medium, cells were washed 3 times with Advanced RPMI containing an antibiotic-antimycotic and 2 mM L-glutamine (medium A), and the medium was switched to fresh medium A. After incubation for 3 days, medium A was collected and centrifuged at 2000 × *g* for 10 min at room temperature. To thoroughly remove cellular debris, the supernatant was centrifuged again at 12,000 × *g* for 30 min at room temperature or filtered through a 0.22-μm filter (Millipore). The conditioned medium (CM) was then used for miRNA extraction and functional assays as well as exosome isolation.

For exosome preparation the CM was ultracentrifuged at 110,000 × *g* for 70 min at 4 °C. The pellets were washed with 11 ml of PBS, and after ultracentrifugation they were resuspended in PBS. The exosome fraction was measured for its protein content using the Micro BCA Protein Assay kit (Thermo Scientific, Wilmington, DE).

*Isolation of MicroRNAs*—Isolation of extracellular and cellular miRNAs was performed using the miRNeasy Mini Kit (Qiagen). Two hundred microliters of conditioned medium or cell lysate was diluted with 1 ml of Qiazol Solution. After 5 min of incubation, 10 μl of 0.1 nM cel-miR-39 was added to each aliquot followed by vortexing for 30 s. Subsequent extraction and filter cartridge work were carried out according to the manufacturer's protocol.

*Quantitative Real Time PCR (QRT-PCR)*—The method for QRT-PCR has been previously described (7). PCR was carried out in 96-well plates using the 7300 Real Time PCR System (Applied Biosystems). All reactions were done in triplicate. All TaqMan MicroRNA Assays were purchased from Applied Biosystems. Cel-miR-39 and RNU6 were used as an invariant control for the CM and cells, respectively.

*Immunoblot Analysis*—SDS-PAGE gels, SuperSep Ace 5–20% (194–15021) (Wako), were calibrated with Precision Plus Protein Standards (161–0375) (Bio-Rad), and anti-KRAS (1:100), anti-ERK5 (1:1000), anti-CD63 (1:200), and anti-actin (1:1000) were used as primary antibodies. The dilution ratio of each antibody is indicated in parentheses. Two secondary antibodies (peroxidase-labeled anti-mouse and anti-rabbit antibodies) were used at a dilution of 1:10,000. Bound antibodies were visualized by chemiluminescence using the ECL PLUS Western blotting detection System (RPN2132) (GE Healthcare), and luminescent images were analyzed by a LuminoImager (LAS-3000; Fuji Film, Inc.). Only gels for CD63 (BD Biosciences) detection were run under non-reducing conditions.

*Plasmids*—The primary-miR-143 expression vector was purchased from TaKaRa BIO. For luciferase-based reporter gene assays, pLucNeo was constructed by inserting a firefly luciferase gene derived from the pGL3-control (Promega) into the pEYFP-1 vector (Clontech) at BglII and AflII sites. The sensor vector for miR-143 was constructed by introducing tandem binding sites with perfect complementarity to miR-143 separated by a four-nucleotide spacer into the NotI site of psiCHECK2 (Promega). The sequences of the binding site are as follows: 5′-AAACCTAGAGCGGCCGCGAGCTACAGTG-CT***TCATCTC***AAAGAATTCTTGAGCTACAGTGCT***TCA-TCTC***AGCGGCCGCTGGCCGCAA-3′ (sense) and 5′-TTG-CGGCCAGCGGCCGCTGAGATGAAGCACTGTAGCTC-AAGAATTCTTTGAGATGAAGCACTGTAGCTCGCGGC-CGCTCTAGGTTT-3′ (antisense). The "seed" sequence of miR-143 is indicated by bold italics. In a mutated miR-143 sensor vector, the seed sequence, TCATCTC, was displaced with GACGAGA. All the plasmids were verified by DNA sequencing.

*Transient Transfection Assays*—Transfections of 10 nM miR-143 mimic and 3 nM anti-miR-143 were accomplished with the DharmaFECT Transfection Reagent (Thermo Scientific) according to the manufacturer's protocol. The total amounts of miRNAs for each transfection were equally adjusted by the addition of NC1 and anti-NC, respectively.